Yale University
EliScholar – A Digital Platform for Scholarly Publishing at Yale

Yale Medicine Thesis Digital Library | School of Medicine

11-9-2009

COPY NUMBER VARIANT ANALYSIS OF PATIENTS WITH MALFORMATIONS OF CORTICAL DEVELOPMENT

Luis Kolb

Follow this and additional works at: http://elischolar.library.yale.edu/ymtdl

Recommended Citation
Kolb, Luis, "COPY NUMBER VARIANT ANALYSIS OF PATIENTS WITH MALFORMATIONS OF CORTICAL DEVELOPMENT" (2009). *Yale Medicine Thesis Digital Library*. 190.
http://elischolar.library.yale.edu/ymtdl/190

This Open Access Thesis is brought to you for free and open access by the School of Medicine at EliScholar – A Digital Platform for Scholarly Publishing at Yale. It has been accepted for inclusion in Yale Medicine Thesis Digital Library by an authorized administrator of EliScholar – A Digital Platform for Scholarly Publishing at Yale. For more information, please contact elischolar@yale.edu.

COPY NUMBER VARIANT ANALYSIS OF PATIENTS WITH MALFORMATIONS OF CORTICAL DEVELOPMENT

A Thesis Submitted to the

Yale University School of Medicine

in Partial Fulfillment of the Requirements for the

Degree of Doctor of Medicine

by

Luis Kolb

2009

ABSTRACT

COPY NUMBER VARIANT ANALYSIS OF PATIENTS WITH MALFORMATIONS OF CORTICAL DEVELOPMENT.

Luis Kolb, Kaya Bilguvar, Michael Di Luna, Chris Mason, Yasar Bayri, Ali Ozturk, Zulfikar Ayer, Nikhil Nayak, and Murat Gunel. Department of Neurosurgery, Yale University School of Medicine, New Haven, CT.

Copy Number Variants (CNVs) are DNA fragment that are approximately 1 kilobase (kb) to several megabases for which copy-number differences have been revealed by comparison of two or more genomes. The Human Genome project has led to the identification of close to 1500 of these variable regions covering 12% of the human genome. Even though many of these variants are considered to be benign, some of these genomic rearrangement have been found to be disease causing, including several nervous system disorders such as Charcot-Marie-Tooth, Williams-Beuren Syndrome, and Prader-Willi syndrome.

In this study we have performed copy number variant analysis on 252 patients with cortical malformations. Cortical malformations represented in our cohort included patients with cortical dysplasia (95), lissencephaly (33), heterotopia (10), pachygyria (8), and polymicrogyria (20), among other diseases.

Two disease-causing copy number variants were identified, and those two diseases are the focus of this manuscript: a diffuse villous hyperplasia of the choroid plexus, and cerebellar atrophy with pachygyria.

Diffuse villous hyperplasia of the choroid plexus is a rare cause of hydrocephalus not amenable to shunting alone. Tetrasomy of the short arm of Chromosome 9 was identified using high-resolution genomic array mapping, broadening the phenotype of this described entity to include diffuse villous hyperplasia of the choroid plexus.

Congenital ataxia with cerebellar hypoplasia is a heterogeneous group of disorders that presents with motor disability, hypotonia, incoordination, and impaired motor development. A homozygous deletion in the VLDLR gene was identified using high density single nucleotide polymorphism (SNP) micro arrays in a Turkish family with two siblings affected with cerebellar atrophy and pachygyria. Previous identification of *VLDLR* mutations in a Turkish family with quadrupedal gait led to various speculations ranging from “reverse evolution” to cultural influences. Discovery of disease causing homozygous deletions in a new Turkish family, which maintained bipedal movement, constitutes significant evidence against these speculations.

ACKNOWLEDGMENTS

It is a pleasure to thank the many people who made this thesis possible.

First, I would like to thank my mentor Murat Gunel for given me the opportunity, mentorship, and support during the past years.

I would also like to thank Kaya Bilguvar, Micheal DiLuna, Chris Mason, and Yasar Bayri for their significant contributions to this manuscript.

I wish to thank Angiliki Louvi and the Gunel and State lab for their continual help and support during this endeavor.

I wish to finally thank my parents, siblings, and friends for all their patronage.

This project was funded by the NIH and the Program on Neurogenetics at Yale University School of Medicine.

TABLE OF CONTENTS

INTRODUCTION

Malformations of cortical development (MCD) are an important cause of epilepsy and developmental delay.[1] It is estimated that up to 40% of children with refractory epilepsy have a cortical malformation.[2] This group of disorders is composed of a large spectrum of abnormalities related to cortical development with varied genetic etiologies, anatomic abnormalities, and clinical manifestations. While prior to 1980 many of these disorders were solely diagnosed at autopsy, the use of magnetic resonance imaging (MRI) has dramatically improved our ability to recognize these diseases.

Cerebral cortical development involves a series of highly organized and complex events, broadly including neural stem cell proliferation, migration, and neuronal differentiation. Disruptions of any of these various stages may result in malformations of cortical development. Disorders due to abnormalities of cell proliferation may cause microcephaly (small brain), megalencephaly (large brain), or cortical dysplasia (focal areas of abnormal neuronal architecture). Disorders of initiation of neuronal migration may result in periventricular heterotopia (PH) (abnormal nodules of neurons located along the ventricular wall). Disorders of later migration and motility cause disruption of the normal 6-layered cortex, such as classic lissencephaly (smooth brain) and subcortical band heterotopia (heterotopic neurons located midway between the surface of the brain and lateral ventricles). Finally, disorders of neuronal arrest can result in neurons that fail to stop upon reaching their intended destination in the cerebral cortex and over migrate

onto the cortical surface as is the case in cobblestone lissencephaly. Although cortical development has been separated into these stages, there is a significant overlap with no clear juncture, and many abnormalities may cause dysfunction at more than one level. Thus, malformation syndromes are typically classified based on the earliest assumed disruption of development. These concepts serve as the basis for the latest classification scheme for these disorders.[3] (Table 1)

The pathogenesis of these malformations is thought to be multifactorial. Genetic mutations or environmental insults, acquired either in utero at different stages of brain development or during the perinatal or postnatal period after corticogenesis, may all contribute to the development of these diseases. [4, 5] The extent of the malformation syndrome will be determined by the timing, severity, type of environmental influences, and genetic factors.

Table 1: Classification of diseases of cortical development.

- **I. Malformations due to abnormal neuronal and glial proliferation or apoptosis**
  - a. Decreased proliferation / increased apoptosis or increased proliferation / decreased apoptosis – abnormalities of brain size
    - i. Microcephaly with normal to thin cortex
    - ii. Microlissencephaly (extreme microcephaly with thick cortex)
    - iii. Microcephaly with extensive polymicrogyria
    - iv. Macrocephalies
  - b. Abnormal proliferation (abnormal cell types)
    - i. Nonneoplastic
      1. Cortical hamartomas of tuberous sclerosis
      2. Cortical dysplasia with balloon cells
      3. Hemimegalencephaly
    - ii. Neoplastic (associated with disordered cortex)
      1. Dysembryoplastic neuroepithelial tumor
      2. Ganglioglioma
      3. Gangliocytoma
- **II. Malformations due to abnormal neuronal migration**
  - a. Lissencephaly / subcortical band heterotopia spectrum
  - b. Cobblestone complex / congenital muscular dystrophy syndromes
  - c. Heterotopia
    - i. Subependymal (periventricular)
    - ii. Subcortical (other than band heterotopia)
    - iii. Marginal glioneuronal
- **III. Malformations due to abnormal cortical organization (including late neuronal migration)**
  - a. Polymicrogyria and schizencephaly
    - i. Bilateral polymicrogyria syndromes
    - ii. Schizencephaly (polymicrogyria with clefts)
    - iii. Polymicrogyria or schizencephaly as part of multiple congenital anomaly / mental retardation syndromes
  - b. Cortical dysplasia without balloon cells
  - c. Microdysgenesis
- **IV. Malformations of cortical development, not otherwise classified**
  - a. Malformations secondary to inborn errors of metabolism
    - i. Mictochondrial and pyruvate metabolic disorders
    - ii. Peroxisomal disorders
  - b. Other unclassified malformations
    - i. Sublobar dysplasia
    - ii. Others

Adapted from Barkovich et al. [3].

Work in determining the genetic basis of various MCD has given us greater insight and understanding into the underlying pathophysiology of these disorders. Different mutations of the same gene can cause different phenotypes, likely based on the degree of protein dysfunction (so termed genotype-phenotype correlation). Loss or disruption of the functional domains within a gene in some cases is enough to determine the phenotype of the disorder. Alternatively, specific mutations in a given gene can also lead to a gain of function for the aberrant protein. Mosaicism can occur when the mutation is present in a subpopulation of cells, whereas germ line mutations typically lead to expression of the mutant gene in all cells. Functional mosaicism occurs due to X-inactivation in which the mutation is present on 1 X chromosome but not the other. The mutant gene is then expressed only in cells in which the mutant gene is found on the active X chromosome, explaining why affected females often are less severely affected than males. An understanding of some of the underlying genetic basis for these disorders will play an important role in genetic counseling of affected individuals and their families.[1]

Traditionally, genetic diseases are classified as chromosomal (numerical or structural); Mendelian (or single gene disorders); multifactorial/polygenic complex diseases; congenital anomalies; and diseases associated with specific mitochondrial gene mutations. Apart from chromosomal disorders, essentially all genetic disorders result from either some sort of alteration or mutation occurring in a specific gene (single gene diseases) or from the involvement of multiple loci spread across the human genome (polygenic disorders). Each of these disorders has major impact on patients. The majority of chromosomal disorders affect patients before birth and carry serious health burden

throughout childhood and during the early years of life. Single gene diseases peak around mid-childhood and pose a real medical and health burden from the perinatal period to adult age. In contrast polygenic/multifactorial disorders present late, with the exception of developmental anomalies requiring active multi-disciplinary care during the early life.[6]

Genetic studies on human disease have been for long time limited to the investigation of single gene diseases. These monogenic disorders tend to be rare, severe and follow clear patterns of inheritance that can be accurately traced through generations. Once these diseases were adequately phenotyped, specific candidate genes within linkage intervals were searched for mutations in the patients and family members. More than 2000 diseases have been identified in this manner, with most of these diseases caused by single base mutations that lead to missense or nonsense mutations according to the Database of Genomic Variants (http://projects.tcag.ca/variation/). For example, four autosomal recessive genes are associated with microcephaly: *Microcephalin*[7], *ASPM* (abnormal spindle-like, microcephaly-associated)[8 9], *CDK5RAP2* (CDK5 regulatory subunit-associated protein 2) [10], and *CENPJ* (centromere protein J) [10]. These genes seem to play a role in cell division during neurogenesis at the ventricular neuroepithelium by playing an important role in the regulation of microtubules and cell cycle progression during cell division.[10 11-13] X-Linked mutations in *FLNA* [14-16]and autosomal recessive mutations in *ARFGEF2* (ADP-ribosylation factor guanine exchange factor 2) [17] are associated with Periventricular Heterotopia; and Subcortical band heterotopia is caused by mutations in the microtubule-associated *DCX* gene[18]. Several genes have been identified giving rise to classic lissencephaly: *LIS1* (Lissencephaly1, autosomal dominant),[19] *DCX* (Doublecortin,

X-linked dominant),[20] *TUBA1A* (Tubulin alpha 1A, autosomal dominant),[21, 22] *ARX* (Aristaless, X-linked dominant),[23] and *RELN* (Reelin, autosomal recessive) [23], with causative genes having characteristic differences in the clinical and radiographic presentation. Cobblestone lissencephaly follows an autosomal recesive intheritance pattern and has been associated with *POMT1*[24], *POMT2*[25] , *POMGnT1*[26], and *Fukutin*[27]; genes involved in the glycosylation of α dystroglycan, a receptor for multiple extracellular molecules that maintains the stability of the cell surface. Bilateral frontal and parietal polymicrogyria seem to be associated with mutations in the *G-protein-coupled receptor gene (GPR56)*[28, 29], assumed to play a role in the regional organization of the brain (Table 2).

Table 2: Genetic basis of malformations of cortical development

Syndrome	Locus	Gene	Protein
Autosomal recessive periventricular heterotopia / micrcocephaly	8p23	MCPH1	Microcephalin
Autosomal recessive periventricular heterotopia / micrcocephaly	1q31	ASPM	Abnormal spindle-like microcephaly
Autosomal recessive microcephaly	9q34	CDK5RAP2	CDK-5 regulatory-associated protein 2
Autosomal recessive microcephaly	13q12.2	CENPJ	Centromere-associated protein J
Autosomal recessive periventricular heterotopia / micrcocephaly	20q13.13	ARFGEF2	ARFGEF2
Amish lethal microcephaly	17q25.3	SLC25A19	Nuclear mitochondrial deoxynucleotide carrier
Seckel syndrome 1	3q22-q24	ATR	Ataxia telangiectasia and Rad3 related protein
Isolated lissencephaly sequence	Xq22.3-q23	DCX-XLIS	DCX
Subcortical band heterotopia	Xq22.3-q23	DCX-XLIS	DCX
Miller-Dieker syndrome	17p13.3	Several contiguous	PAFAH1B1, 14-3-3 and others
Isolated lissencephaly sequence	17p13.3	LIS1	PAFAH1B1
Subcortical band heterotopia	17p13.3	LIS1	PAFAH1B1
Lissencephaly with cerebellar hypoplasia	7q22	RELN	Reelin
X-linked lissencephaly with abnormal genitalia	Xp22.13	ARX	Aristaless-related homeobox protein
Fukuyama congenital muscular dystrophy	9q31	FCMD	FCMD or Fukutin

Table 2: Genetic basis of malformations of cortical development (Cont.)

Syndrome	Locus	Gene	Protein
Muscle-eye-brain disease	1p33-p34	POMGnT1	Unknown
Muscle-eye-brain disease	19q13.3	FKRP	Fukutin-related protein
Congenital muscular dystrophy	19q13.3	FKRP	Fukutin-related protein
Congenital muscular dystrophy	22q12.3-q13.1	LARGE	
Walker-Warburg syndrome	9q34.1	POMT1	O-Mannosyl-transferase 1
Walker-Warburg syndrome	19q13.3	FKRP	Fukutin-related protein
Walker-Warburg syndrome	9q31	FCMD	FCMD
Bilateral periventricular nodular heterotopia	Xq28	FLNA	Filamin-A
Bilateral periventricular nodular heterotopia + microcephaly	20q13.3	ARFGEF2	BIG2
Bilateral periventricular nodular heterotopia	5p15	Unknown	Unknown
Tuberous sclerosis chromosome 1	9q32	TSC1	Hamartin
Tuberous sclerosis chromosome 2	16p13.3	TSC2	Tuberin
Bilateral frontoparietal polymicrogyria	16q13	GPR56	Unknown
Warburg microsyndrome 1	2q21.3	RAB3GAP	
Bilateral perisylvian polymicrogyria	Xq28	Unknown	Unknown

Adapted from Barkovich et al. [3].

Recent advances in molecular genetics have enabled us to identify specific groups of disorders that result from previously uncharacterized mechanisms. Often these disorders do not conform to the standard basic principles of genetics, and involve specific areas of the human genome. A broad term 'genomic disorders' has been coined to describe these conditions[6]. Broadly, this group of disorders can be subdivided into disorders in the genome architecture, trinucleotide repeat disorders, chromosome breakage disorders, non-disjunction disorders, and complex genomic diseases. [6]

These disorders follow unusual non-traditional inheritance mechanisms that involve genomic regions that directly or indirectly influence the regulation and expression of one or more genes manifesting in complex phenotypes. The evolution of the mammalian genome has resulted in the duplication of genes, gene segments and repeats of gene clusters.[30] This aspect of genome architecture provides recombination hot spots between non-homologous regions of chromosomes that are distributed across the whole genome. These genomic regions become susceptible to further DNA rearrangements that may be associated with abnormal phenotypes. [31-34]

These 'hotspot' regions usually lie within genomic regions referred to as Low Copy Number Repeats (LCR). LCR are region specific DNA blocks usually 10 to 300 kilobases (kb) in size and of > 95% to 97% similarity to each other that usually map to two or three locations in the genome.[35-37] It is estimated this regions account for ~5% of the human genome. They can contain any standard constituent of genomic DNA, including gene families, gene containing structural motifs, or sequences of unknown

function present in clusters or dispersed through the genome. Examples include the HLA and related genes, actins, zinc-finger genes, and the CRI-S232 sequence family. LCRs are distinguished from highly repetitive sequences in the human genome by their high degree of sequence similarity and large numbers, and often appear to locate preferentially near centromeres and telomeres in human chromosomes.[38, 39]

The term 'genome architecture disorder' refers to a disease that is a result of an alteration of the genome that results in complete loss, gain or disruption of the structural integrity of dosage sensitive genes.[40, 41] Disruption in the function of dosage sensitive gene may result from number of mechanisms including gene interruption, gene fusion, position effect, unmasking of a recessive allele, presence of a functional polymorphism, and gene transvection effect.[6] Notable examples include a number of microdeletion / microduplication syndromes such as Williams- Beuren syndrome [42], Prader-Willi syndrome[43], Angelman syndrome[44], Smith Magenis syndrome[45], Potoki Lupski syndrome[45], DiGeorge syndrome[46], and Neurofibromatosis type 1[47]. (Table 3) In these conditions there is a critical rearranged genomic segment flanked by large (usually > 10 kb), highly homologous low copy repeat structures that can act as recombination substrates.[48] Meiotic recombination between non-allelic LCR copies, also known as non-allelic homologous recombination, can result in deletion or duplication of the intervening segment[6]. The phenotype of these disorders is distinctly recognizable with particular clinical and facial dimorphic features.

An increasing number of Mendelian diseases are being recognized to result from recurrent inter and intra chromosomal rearrangements involving unstable genomic regions.[6] These genomic regions have been shown to be predisposed to non-allelic homologous recombination by proximity to 'hot spot' genomic segments.[49] Large genomic deletions and duplications have been reported as being pathogenic in cases of various diseases, such as Duchenne and Becker muscular dystrophies, familial breast cancer, hereditary nonpolyposis colorectal cancer, and Williams-Beuren syndrome. (Table 4) Previously, our lab reported a homozygous microdeletion in the *parkin* gene (*PARK 2*) in a Turkish family in which six members were afflicted with autosomal recessive Parkinsonism. [50] Mutations in the *PARK2* gene had been previously shown to be associated with early-onset Parkinson's disease[51].

Even though traditionally when one considers what constitute 'genetic diseases' one usually refers to traits inherited in a Mendelian fashion and resulting from base pair changes that alter an encoded protein's structure, function and regulation, clinical conditions observed in genetics are sporadic in >97% of the cases. Often these cases are not due to mutant genes, but instead result from genomic copy number variations.[52] 2-3% of children are born with a major birth defect and often these are sporadic in nature.[53, 54] Chromosomal anomalies, such as trisomy 21, have been shown to be responsible for birth defects in ~0.2% of live births.[55] Recessive traits are thought to compose a similar proportion .[55] *De novo* point mutations are also known to cause sporadic disease as is in common cases of achondroplasia, neurofibromatosis type 1, and tuberous sclerosis, as well as multiple other diseases.[52]

Direct estimates of human per-nucleotide rates for spontaneous mutations have been estimated to between 0.5 x 10^{-8} to 3 x 10^{-8} from the per-locus mutation rates and sequences of *de novo* nonsense nucleotide substitutions, deletions, insertions, and complex events causing autosomal dominant and X-Linked diseases[56]. In the context of the 3 x10^{9} bp haploid human genome, this rate corresponds to ~60 new mutations per germ cell, with male germ cells having more than female germ cells as most point mutations presumably represent DNA replication or repair errors. Approximately 2% (2.4) of them will affect exonic sequences, thus about two exons (and thus genes) have a de novo base-pair change. Of these, at least one third are likely to have little effect as they would lie in the third position of a codon.[52] Thus, it seems paternal age affect is the most likely cause of 'sporadic cases' often being found among the last-born children of a sibship.[57, 58]

In contrast, the *de novo* locus-specific mutation rates for genomic rearrangements has been calculated to be between 10^{-6} and 10-^{4} from sporadic microdeletion syndromes, common autosomal dominant or X-Linked disease prevalence rates, by direct measurement by either sperm PCR at the alpha globin or t(11;22) recombination breakpoint sites, and by genomic assays comparing child to parents in trios.[52] This rate is at between 2 and 4 orders of magnitude (100 to 100,000 fold) greater than observed rates of *de novo* locus-specific mutation point mutations. It appears that genomic rearrangements are more common than point mutations, and that the mechanisms causing them are more prevalent as well.

There appears to be three primary recombination mechanisms responsible for generating deletions and duplications that cause genomic rearrangements that can be associated with genomic disorders.[49] Nonallelic homologous recombination (NAHR), described above, appears to be the more frequent mechanism for specific regions of the genome that have architecture that favors genomic instability, and has been proposed as the main mechanism for genomic rearrangements due to the proximity of most genomic rearrangements to low copy repeats[40, 59]. This seems to be especially true for most of the recurrent rearrangements that share a common size, show clustering of breakpoints, and recur in multiple individuals. In this process, non-allelic copies of LCRs, instead of the copies at the usual allelic positions, are aligned in meiosis or mitosis. This 'misalignment' results in genomic rearrangements in the progeny cells. When the two LCRs are located on the same chromosome and in direct orientation, the resulting rearrangement is either a deletion or duplication. When the LCRs are in the same chromosome but in opposite orientation, the process results in inversion of the fragment flanked by them. Non-allelic homologous recombination on different chromosome results in chromosomal translocation.[41]

Nonhomologous end joining (NHEJ) and the Fork Stalling and Template Switching (FoSTeS) have been proposed as the other two mechanisms responsible for genomic rearrangements, especially for the non-recurrent cases. Non-recurrent rearrangements are of different sizes in each patient, but may share a small region of overlap whose change in copy number may result in shared clinical features among different patients.[59] These

non- recurrent rearrangements might be stimulated by low copy repeat regions, as well as might be mediated by highly homologous repetitive sequences such as the Alu, and LINE sequences.

Nonhomologous end joining (NHEJ), which plays a critical role in V D J recombination - the process by which B-cell and T-cell diversity is generated, is one of the two major mechanisms used by eukaryotic cells to repair both physiological and pathological double stranded breaks (DSB).[60, 61] NHEJ is considered to be the major mechanism responsible for joining translocated chromosomes in cancer.[61] The process proceeds in four steps: detection of DSB; molecular bridging of both broken DNA ends; modification of the ends; and ligation of the ends. Sequence studies on non-recurrent deletions in the DMD gene and the PLP1 gene, as well as duplications on the PLP1 have found evidence these genomic rearrangements are caused by the NHEJ mechanism.[62, 63] It has been proposed that the first step of the rearrangement is when a single DSB occurs in one strand; followed by the broken ends being invaded and copied from the sister chromatid; and finally the ends being rejoined via NEHJ.

Some rearrangements are far more complex than those able to be explained by NAHR and NEHJ mechanisms. To explain these more complex events, the Fork Stalling and Template (FoSTees) model has been proposed.[64] In this model, during DNA replication the DNA replication fork stalls at one position causing the lagging strand to disengage from the original template, and transfer and anneal to another replication fork in physical proximity. The DNA replication process then ‘primes’ again, and continues DNA

synthesis[65]. Switching to another folk located downstream would result in a deletion, while switching to a fork upstream would result in duplication. The process of disengaging, invading/annealing, synthesis/extension could occur multiple times resulting the observed complex rearrangements.[49] Although still very limited, preliminary data implies that FoSTeS might be a major mechanism of duplication, and might have also been the driving force in the origin of Low Copy Repeats.

Eighteen years ago it became evident that genomic rearrangements and gene dosage effects, rather than the classical model of coding region DNA sequence mutations, could be responsible for nervous system diseases when a duplication in CMT1A was discovered to be responsible for Charcot-Marie Tooth neuropathy type 1a, a common, autosomal dominant adult-onset neurodegerative disease.[66, 67] Now, several neurodegenerative and neurodevelopmental disorders are known to be caused by disparate recurrent and non-recurrent genomic rearrangements.[68] These genomic disorders include peripheral and central nervous system neuropathies, well-recognized syndromes with characteristic phenotypes, and also a growing group of psychiatric illnesses. Some of these disorders include the deletion in PMP22 causing hereditary neuropathy with liability to pressure palsies (HNPP), and some of the recurrent microdeletion disorders previous mentioned like Williams-Beuren Syndrome[42], Angelman syndrome[44], and Prader Willi syndrome[43].

Several new genomic disorders caused by genomic rearrangements leading to nervous system diseases have been recently recognized. Duplications of the genomic region deleted in Williams-Beuren syndrome have been described, with patients characterized by prominent speech delay.[42, 69, 70] Tandem duplications of *LMNB1* have been reported to cause adult-onset autosomal dominant leukodystrophy[71], and duplications in *PAFAH1B1/LIS1* and *YWHAE* –genes deleted in lissencephaly *(PAFAH1B1/LIS1 alone)* and Miller-Dieker syndrome (both) were found in patients with developmental delay[72, 73]. Finally, two new microdeletion syndromes have been described in 17q21.31[74, 75] and 15q13.3[76], and the reciprocal duplications, have been recognized.

With the advent of the completion of the Human Genome, thousands of single nucleotide polymoprhisms have been discovered and their use as common polymorphic markers has revolutionized genome-wide studies. A SNP is a variation of a single nucleotide in the DNA sequence that occurs between members of the same species. SNPs may fall within the coding sequence of genes, intronic sequence of genes, or in intergenic regions. Some SNPs may contribute directly to disease phenotype by altering the gene function, especially those lying within the coding sequences. The majority, though, are located outside protein coding regions.[77]

There are approximately 10 million SNPs with a minimum allele frequency of 1% that have been discovered spread throughout the genome.[78] A minimum allele frequency of 1%, which means the rarer allele occurs with a frequency of at least 1% of the population, is commonly used as a cutoff when considering a single base change as a rare variant or

polymorphisms. Assays have been developed using SNPs as markers that are cheap and easy to perform and take advantage of SNPs being numerous, frequent and stable. These assays are increasingly being used in genome wide studies of individuals, families and populations.

A large, well-characterized collection of SNPs has become increasingly important in the discovery of DNA sequence variations that affect biological function. A block of associated SNPs in a region of the genome is called a haplotype. Many parts of the genome exist with distinctive areas of common haplotypes, which account for most of the individual variation within a population. The International HapMap Project is an international collaboration with the goal of developing a haplotype map of the human genome, which will describe the common patterns of human genetic variation.[79] In many ways this is information is thought to simplify the human genome so that instead of having to scan through 10 million SNPs to explain human variation, it may be possible to breakdown the genome into specific areas of increase variation that can be specifically tagged with SNPs, thereby reducing the amount of genotyping required. The current phase II HapMap characterizes over 3.1 million human SNPs from four geographically diverse populations[80].

In addition to the identification of thousands of SNPs, the Human Genome project has led to the identification of a range of other DNA sequence variations such as insertions, deletions, and translocations of various segments of chromosomes.[81] The term Copy Number Variant (CNV) was coined to describe a copy number change involving a DNA

fragment that is approximately 1 kilobase (kb) to several megabases for which copy-number differences have been revealed by comparison of two or more genomes. These changes can be copy-number gains (duplications or insertional transpositions, losses (deletions), gains or losses of the same locus, or multiallelic or complex rearrangements. This excludes insertions or deletions involving transposable elements. Even though it was well known previous to the Human Genome Project that large duplications and deletions have a mechanistic role in the development of a range of human genetic diseases, it was during the Human Genome Project and subsequent studies that it was appreciated that humans carry a far higher than expected number of CNVs.[82-84] It has been speculated there are close to 1500 variable regions covering 12% of the human genome that equal or even surpass the number of nucleotides affected by SNPs. [85]

CNV discovery will continue. Many of these CNVs are likely to represent benign variants, but proving they do not have phenotypic consequences or that they do not account for normal physical or behavioral traits will be a challenge. It is also a challenge to establish a cause-and-effect relationship for a specific genomic rearrangement and a given phenotype; and even more of a challenge to determine the dosage-sensitive gene or genes within the genomic rearrangement. Regardless, when analyzing genetic disorders, one should consider new mutation. Given that the frequency of de novo structural changes can be four orders of magnitude greater than that of base pair changes, CNV should be considered a potential significant cause of sporadic disease and Mendelian disorders. These diseases include the malformations of cortical development detailed above.

STATEMENT OF PURPOSE & SPECIFIC AIMS

The purpose of this study is to utilize molecular genetics techniques, specifically SNP genotyping, CNV analysis and homozygosity mapping, in order to find genetic mutations that cause diseases of neural development. This manuscript details our studies on our neurogenetics cohort and on two diseases in particular: Cerebellar Atrophy, and Choroid Hyperplasia. Our aim is to uncover the gene mutations that cause these disorders so that we may develop a better understanding of the pathophysiology of these diseases specifically and malformations of neural development generally.

METHODS

Patient Identification and Collection of Blood Samples

Approval for this study was obtained from the Yale Human Investigations Committee (Protocol 7680). The patients afflicted with malformations of cortical development were identified by physicians at Yale New Haven Hospital as well as collaborators at other institutions in the United States and Europe. Diagnosis for each patient was established by the identifying physician based on physical findings, computerized tomography (CT) findings, and/ or magnet resonance imaging (MRI) findings. For patients identified at Yale New Haven Hospital, the author attained consent and collected their blood samples. For patient identified elsewhere, consent was attained and blood samples were collected by the collaborating physicians, and Ethical Committee approval was obtained from each institution.

Isolation of Genomic DNA

Total genomic DNA was isolated from lymphocyte nuclei using a procedure described by Bell et al. [86]. Ten milliliters of blood collected in a heparinized tube and then kept at 4°C was mixed with 90 ml of 0.32 M sucrose / 10 mM TrisHCl (pH 7.5) / 5 mM $MgCl^2$ / 1% Triton X-100 at 4°C to lyse all cells. The nuclei were collected by centrifugation at 1000

X g for 10 min. The nuclear pellet was suspended in 4.5 ml of 0.075 M NaCl / 0.024 M EDTA (pH 8.0) with a Pasteur pipette. Then 0.5 ml of 5% sodium dodecyl sulfate and proteinase K at 2 mg/ml were added and the mixture was incubated for approximately 12 hr at 37°C.

The digest was gently mixed with 5 ml of phenol saturated with 20 mM Tris HCl (pH 8.0). Five milliliters of chloroform / isoamyl alcohol (24:1, vol/vol) was added and gentle mixing was continued. The phases were separated by centrifugation for 15 min at 1000 X g. The upper, aqueous, phase was removed and gently extracted with the chloroform / isoamyl alcohol mixture. After centrifugation, the aqueous phase was removed; 0.5 ml of 3 M sodium acetate and 11 ml of 100% ethanol (at room temperature) were added. The DNA was precipitated by inverting the tube several times and then removed with a Pasteur pipette and placed in 1 ml of 10 mM Tris HCl (pH 7.5) / 1 mM EDTA. The DNA was allowed to dissolve at 4°C. From 10 ml of blood, 20-50 μg of DNA was obtained. In cases where the yield is low, we incubate the DNA at -20°C in the presence of ammonium acetate. Genomic DNA was isolated by the author and laboratory technicians.

Single Nucleotide Polymorphism Genotyping and Quality Control

Single Nucleotide polymorphism genome-wide genotyping was performed on the Illumina plataform 370 Human CNV and the Human610-Quad Beadchip (containing

379.473 and 620,089 SNPs respectively; Illumina, San Diego, CA, USA). All procedures were done according to manufacturer's protocol. Briefly, 200 ng of genomic DNA was amplified, fragmented, and hybridized to the array, and products were fluorescently labeled and scanned with Illumina Beadstation scanner. Raw data was then uploaded in Beadstudio v3.3 genotyping software (Illumina, San Diego, CA, USA) for further analysis. Samples of subjects that had genotype call rates < 97% (n=6), heterozygosity > 37% (n=3) or samples with incorrectly imputed gender (n=0) were excluded. SNP genotyping was performed by laboratory technicians.

CNV Detection

Data was analyzed using BeadStudio v3.3 (Illumina Inc., San Diego, CA). Two metrics were visualized using this tool: B allele frequency and log R ratio. The B allele frequency is the theta value for an individual SNP corrected for cluster position. This parameter provides an estimate of the proportion of times an individual allele at each polymorphism was called A or B. In this setting, an individual who is homozygous for the B allele (BB genotype) would have a score close to 1, an individual homozygous for the A allele (AA) would have a score close to 0, and an individual who is heterozygous (AB) would have a score of approximately 0.5. Significant deviations from these figures in contiguous SNPs are indicative of a CNV. The log R ratio is defined as the log (base 2) ratio of the observed normalized R value for the SNP divided by the expected normalized R value for the SNPs theta value. The expected R value is calculated from the values theta and R,

where R is the intensity of dye labeled molecules that have hybridized to the beads on the array and theta is the ratio of signal at each polymorphism for beads recognizing an A allele to beads recognizing a B allele. The expected R value for any individual at any typed SNP is calculated using a large population of typed individuals. Therefore, the ratio of observed R to expected R in any individual at any SNP gives an indirect measure of genomic copy number. An R value above 1 is indicative of an increase in copy number, and an R value below 1 suggests a decrease (deletion) in copy number. While this metric exhibits a high level of variance for individual SNPs, it does provide a measure of copy number when log R ratio values for numerous contiguous SNPs are visualized. We evaluated both the log R ratio and the B allele frequency plots across the genome in all samples. (Figure 1, Figure 2)

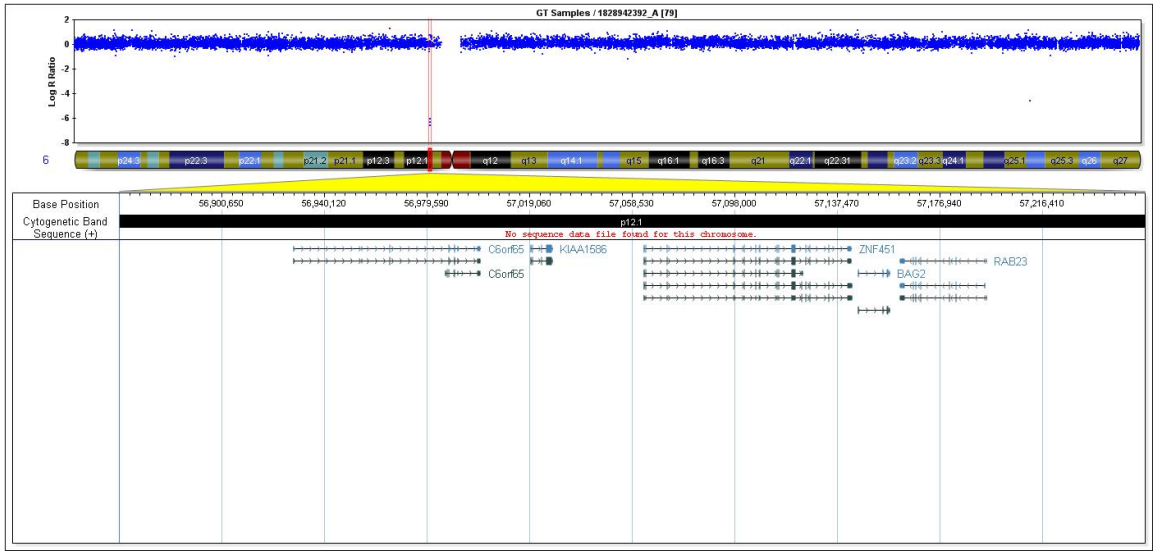

Figure 1: Homozygous Deletion example. Log R ratio plot. Scatter points represent normalized log2 ratios (y) for probes along the chromosome. A segment was considered to be significant if $y > 3$ or $y < -3$. A deletion spanning 2 consecutive probes with $y < -3$ can be appreciated.

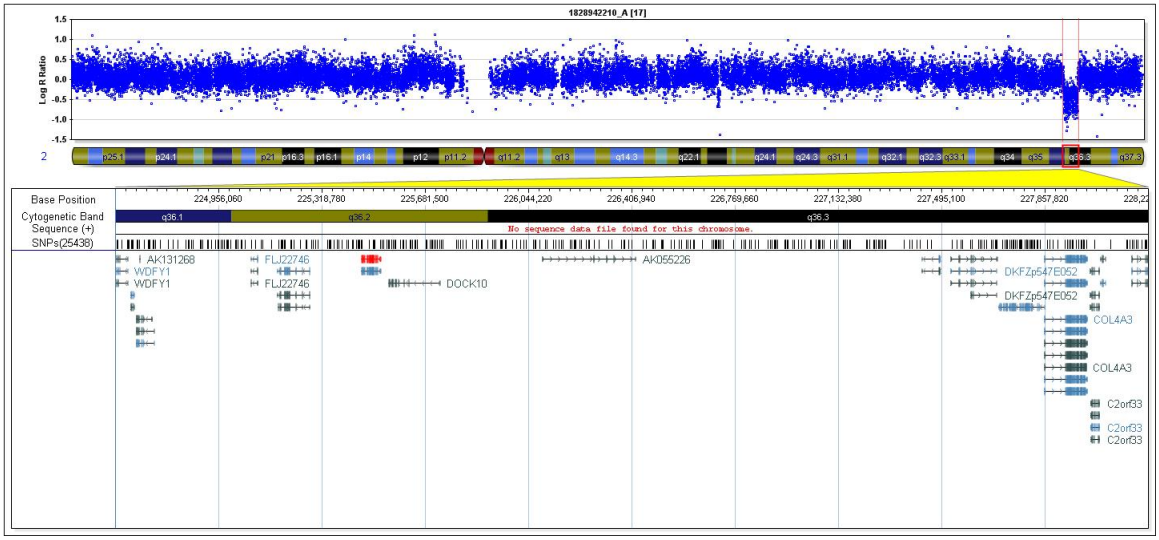

Figure 2: Heterozygous deletion example. Log R ratio plot. Scatter points represent normalized log2 ratios (y) for probes along the chromosome. A segment was considered to be significant if $y > 1.5$ or $y < -1.5$. A deletion spanning 2 kb $y < -1.5$ can be appreciated.

A previously described high-resolution CNV detection algorithm, the PennCNV algorithm [87], was used to infer CNVs from the signal intensity data. This algorithm incorporates multiple sources of information, including total signal intensity and allelic intensity ratio at each SNP marker, the distance between neighboring SNPs, the allele frequency of SNPs, as well as family information when available. We set a threshold at 2 SNPs for homozygous deletions and 10 SNPs for heterozygous deletions to avoid false positive calls. This threshold was previously shown to result in a false positive rate lower than 1% for high-quality samples [87, 88].

To define common and rare CNVs we mapped these CNVs to the UCSC genome browser for comparison with those previously identified in other publications, or with those included in the database of genomic variants (http://projects.tcag.ca/variation). The common and rare CNVs were defined as those that occurred at a frequency of >1% or <1% in general populations. The CNVs which were not detected in control subjects and in the database of genomic variants were considered to be possibly disease causing. Genechip analysis was performed by the author and by laboratory personnel.

Inbreeding Coefficient

Plink software, a whole genome association analysis toolset, was used to calculate the inbreeding coefficient for each individual patient using the B allele signal data.[89] The Inbreeding coefficient is a measure of how close two people are genetically to each other. Plink calculates the inbreeding coefficient based on the observed versus expected number

of homozygous genotypes given a large number of SNPs in a homogeneous sample. Inbreeding coefficient calculations were performed by the author and laboratory personnel.

Homozygosity Mapping

Plink software was used to conduct runs of homozygosity for each individual patient using the B allele signal data.[89] In brief, the Plink algorithm performs a run of homozygosity by taking a window of *X* SNPs and sliding this across the genome. At each window position it determines whether this window looks 'homozygous' enough (yes/no) (i.e. allowing for some number of heterozygous or missing calls). Then, for each SNP, it calculates the proportion of 'homozygous' windows that overlap at that position. It creates a call for segments based on this metric, e.g. based on a threshold for the average. Homozygous runs were performed using the 100 SNP, 1000 kb windows with SNP densities of 1 SNP per 50 kilobases. One heterozygous SNP call and 5 missing SNP calls were allowed per homozygous window. Homozygosity runs were performed by the author and laboratory personnel.

Candidate Gene Mutational Analysis

Exon-intron boundaries of the candidate genes were determined based on the University of California at Santa Cruz (UCSC) Genome Browser (NCBI Build 36.1). PCR primers were designed using PRIMER3 (http://frodo.wi.mit.edu/cgi-bin/primer3/primer3_www.cgi). . The Basic Local Alignment Search Tool (http://www.ncbi.nlm.nih.gov/blast/) was used for these primers. Exon amplicons were amplified and sequenced using standard techniques. Mutational analysis was performed by the author and by laboratory personnel.

Quantitative RT-PCR

Array CNV analysis results were confirmed with quantitative RT-PCR using the standard curve method for absolute quantization. Primers were designed using Primer Express Software, version 2.0 (Applied Biosystems), with the following criteria: amplicon size of 80 to 200/250 bp, GC content of 20 to 80%, no more than two guanines or cytosines in the primer 3' end, and melting temperature (Tm) of 59 to 60°C. Finally, the Basic Local Alignment Search Tool (http://www.ncbi.nlm.nih.gov/blast/) was used for these primers.

The experimental design and calculations were performed as described by Applied Biosystems (User Bulletin #2). To determine copy number changes, fourfold ranges of five different serial dilutions from five pooled normal control DNA samples were used.

In addition, we used 5 ng of genomic DNA from the patient's DNA and pooled normal control DNA. The RT-PCRs were performed in triplicate for each reaction. The 15-µl reactions contained 1X final concentration of Power SYBR Green PCR Master Mix (part number 4367660, Applied Biosystems) and 400 nM of each primer (Invitrogen). Each experiment was performed using a 384-well optical PCR plate and the Applied Biosystems machine (model 7900HT) with default cycling conditions.

A standard curve was created using the calculated threshold cycle of each dilution for each gene. Amplifications were performed on the same diluted samples using primers for the reference and target genes. For all experimental samples, the target quantity was determined from the standard curve and divided by the target quantity of the normal reference DNA. To assess reaction specificity and to verify product identity, melting curve analysis was performed following amplification. We used the standard curves with an efficiency between 90% and 100%, which corresponds to a slope between 23.58 and 23.20. Quantitative PCR was performed by the author and laboratory personnel.

RESULTS

Patient Collection

To this date, 563 patients with malformations of cortical development and syndromic neurodevelopment diseases have been collected from Yale-New Haven Hospital as well as from collaborators in Europe. Of these 563 patients, 252 patients were diagnosed with cortical malformations and were included in this study. Patients within the designation of cortical malformations included patients diagnosed with polymicrogyria (20), schizencephaly (16), developmental anomaly/ dysplasia (39), and broadly as malformations of cortical development not specified (MCD - 95). 130 patients were genotyped on 370k microarray Illumina Human CNV bead chips, while 119 patients were genotyped on the Illumina 610 Quad chips. Beadchip data from six (6) chips with call rates less than 97% was considered to be of poor quality and was excluded from this study. Genotype analysis also revealed three duplicates, which were removed as well. Sex phenotype on the bead chip data for each patient was also cross-matched with the reported sex to validate the integrity of the each patient sample.

A control group composed of forty (40) patients with a diagnosis of renal tubular acidosis and of self-reported consanguinity was also genotyped on 370k Human CNV Illumina bead chips.

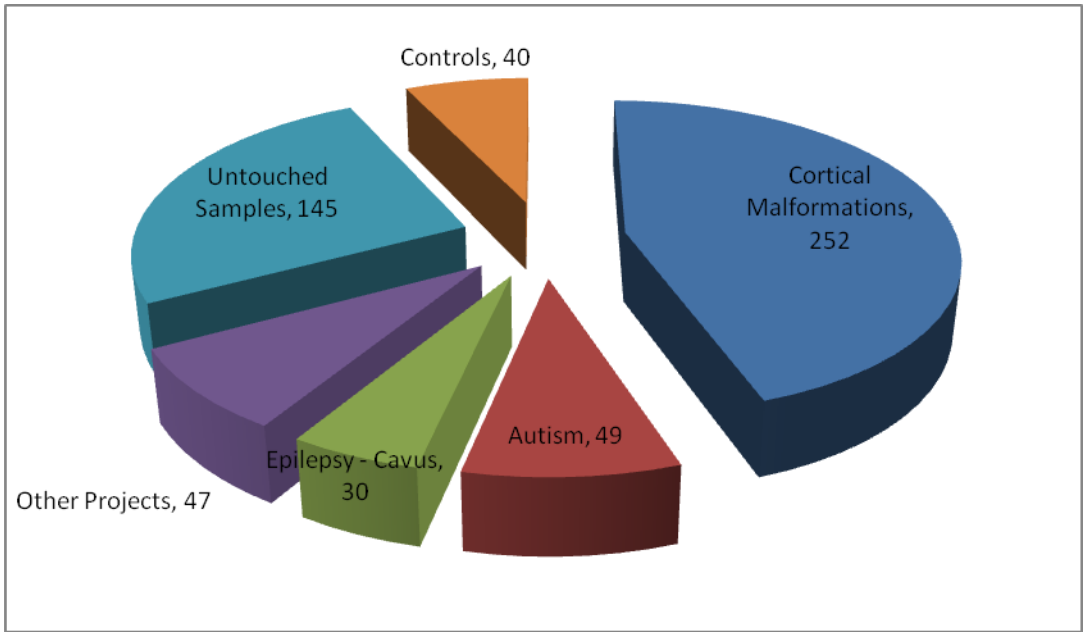

Figure 3: Demographics of Neurogenetics cohort. Total number of patients currently in the cohort is 563 including 252 patients with the diagnosis of cortical malformations.

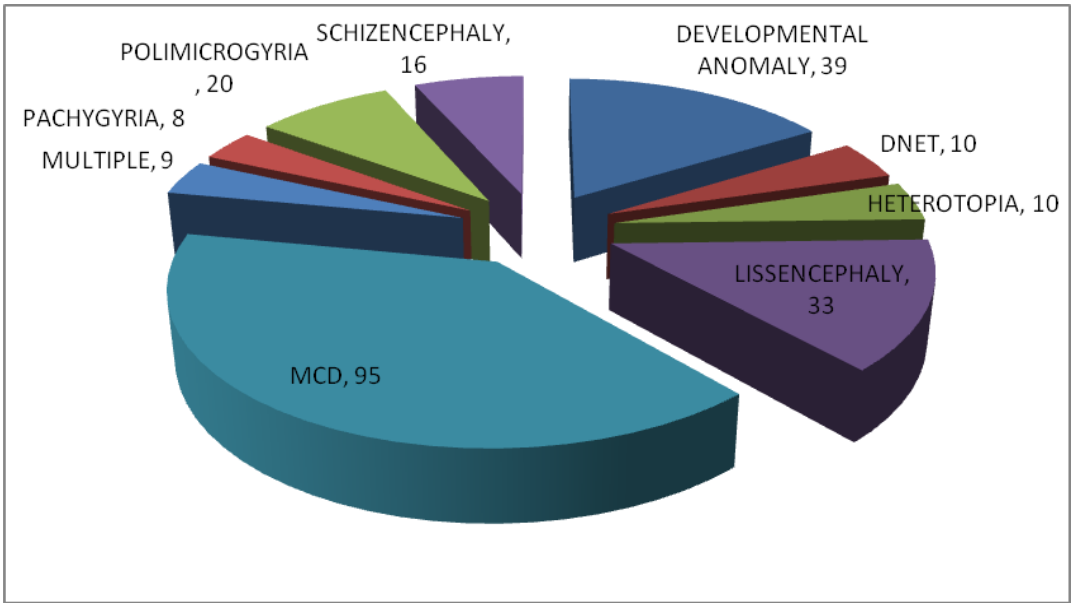

Figure 4: Demographics of patients with cortical malformations within the Neurogenetics Cohort. Total number of patients with cortical malformations is 252. MCD stands for malformations of cortical development not specified.

Copy Number Variant Analysis

Analysis for copy number variants was performed using the Penn CNV algorithm in conjunction with visual inspection of the signal intensities on the Beadstudio plataform. Because of the difference in SNP densities between the two microarray platforms, results are presented divided.

Copy Number Variant Analysis of patients on Illumina 370 Human CNV (N=127)

Copy number variant analysis of the 127 patients genotyped on the Illumina 370 Human CNV bead chips revealed 20 homozygous deletions and 237 heterozygous deletions. Of the 20 homozygous deletions, 7 contain or are within genes. Comparing these seven copy number variants with the published reports and database of human variation eliminates six areas where there is evidence of variability in the general population. One intergenic deletion has not previously been reported.

Copy Number Variant Analysis of patients on Illumina 610 Quad (N=119)

Copy number variant analysis of the 119 patients genotyped on the Illumina 610 Quad Chips revealed 593 homozygous deletions and 840 heterozygous deletions. Of the 593 homozygous deletions, 130 contain or are within genes. Comparing these 130 copy

number variants with the published reports and database of human variation eliminates 128 areas where there is evidence of variability in the general population. Two exonic homozygous deletions are not previously reported, and are located in the VLDLR gene (see below).

Copy Number Variants on Illumina 370 Human CNV

GROUP	# PATIENTS	HZ DELETIONS	HET DELETIONS	NON-REPORTED
CORTICAL DYSPLASIA	5	1	4	0
DEVELOPMENTAL ANOMALY	37	6	35	0
DNET	9	2	6	0
HETEROTOPIA	6	0	5	0
LISSENCEPHALY	22	2	37	0
MCD	20	5	29	1
MULTIPLE	3	2	58	0
POLYMICROGYRIA	17	1	35	0
SCHIZENCEPHALY	8	1	28	0
Total	127	20	237	0

Table 5: Genomic Deletions per Malformations of Cortical Development Sub-group in patients genotyped on Illumina 370 Human CNV Bead Chip. Hz, Homozygous; Het, Heterozygous.

Copy Number Variants on Illumina 610 Quad

GROUP	# PATIENTS	HZ DELETIONS	HET DELETIONS	NON-REPORTED
CORTICAL DYSPLASIA	7	25	35	0
PACHYGYRIA	8	35	58	2
DNET	1	6	4	0
HETEROTOPIA	4	23	25	0
LISSENCEPHALY	8	33	94	0
MCD	74	395	500	1
MULTIPLE	6	24	47	0
POLYMICROGYRIA	2	13	15	0
SCHIZENCEPHALY	8	39	62	0
Total	119	593	840	0

Table 6: Genomic Deletions per Malformations of Cortical Development Sub-group in patients genotyped on Illumina 610 Quad Bead Chips. Hz, Homozygous; Het, Heterozygous.

Copy Number Variant Analysis of Controls

Copy number variant analysis of the 40 controls on the Illumina 370 Bead chips revealed fifteen homozygous deletions and 139 heterozygous deletions. Of the fifteen homozygous deletions, seven are within genes. Comparing these 7 copy number variants with the

published reports and database of human variation eliminates one area of common variability. Five homozygous mutations are known to cause autosomal recessive cases of renal acidosis.

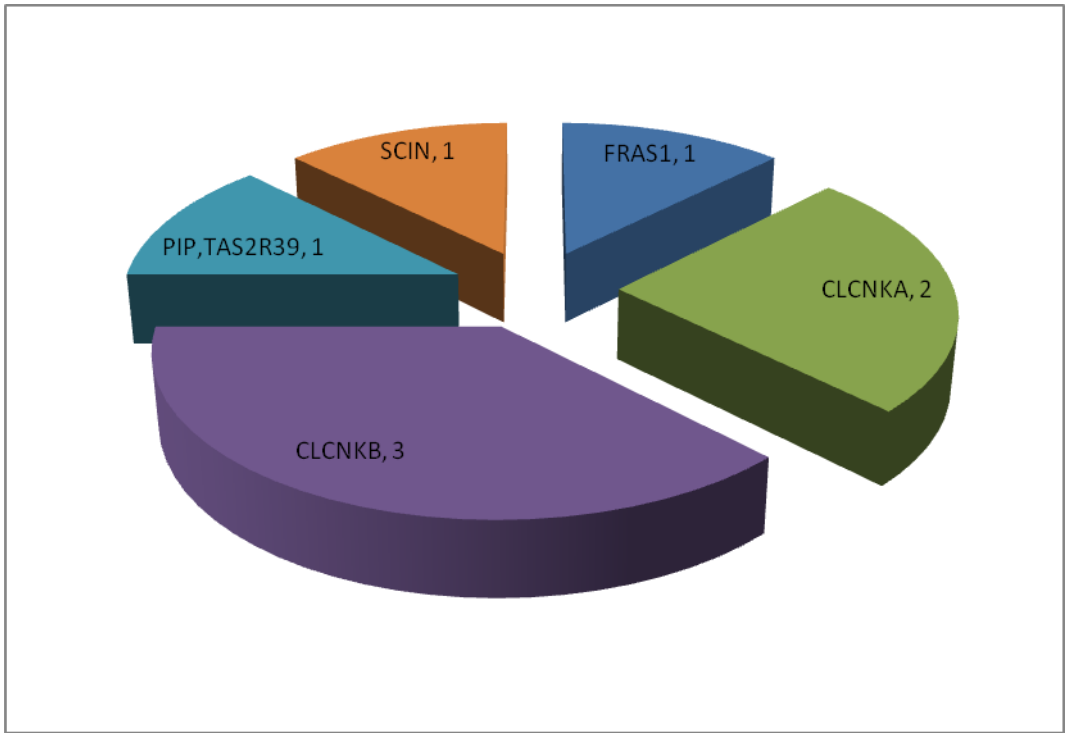

Figure 5: Homozygous deletions within genes in the control population (N = 40). Mutations in CLCNKA and CLCNKB, part of the family of voltage-gated chloride channels, have been associated with Barter's syndrome Type 4, an autosomal recessive disorder defined by hypokalemic metabolic acidosis (OMIM # 602522). Mutations in FRAS1, which encodes a putative extracellular matrix (ECM) protein, is mutated in Fraser syndrome (OMIM #219000).

Copy Number Variant Analysis of Heterozygous Deletions and Amplifications

We are currently in the process of further investigating identified heterozygous deletions as well as amplifications on our samples (results not shown) in order to identify mutations that might be disease causing in our cohort.

Diffuse Villous Hyperplasia of the Choroid Plexus

Background

Diffuse villous hyperplasia of the choroid plexus (DVHCP) is defined as diffuse enlargement of the entire choroid plexus occurring throughout the length of the choroid fissure. DVHCP is a rare cause of hydrocephalus which according to contemporary case reports, is not adequately treated by shunting; It is a rare disorder, having been reported in only a handful of cases[90-94]. Hydrocephalus and congenital malformations of the Dandy-Walker Complex are not often associated with chromosomal abnormalities. Herein we describe a case of a female child born with hydrocephalus, and multiple craniofacial anomalies including cleft palate and lip. CT scan demonstrated DVHCP and hypoplasia of the cerebellar vermis.

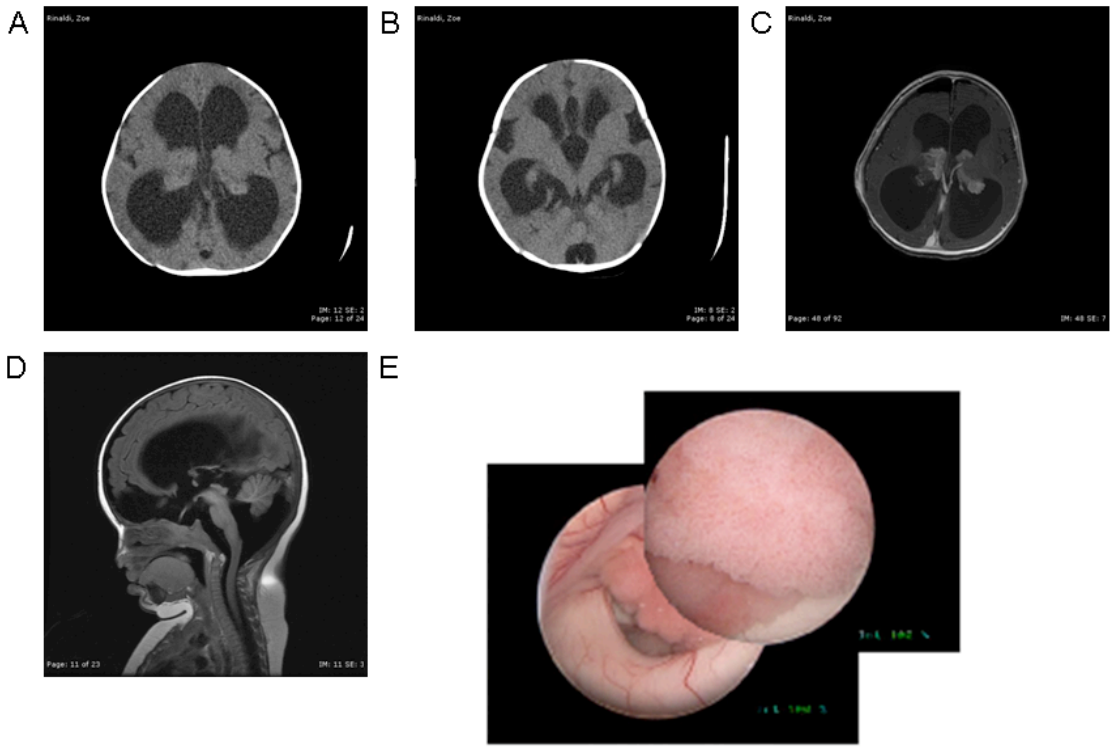

Figure 6: Axial non-contrast head CT. Representative images through the lateral ventricles (A) and third ventricle (B) demonstrate hydrocephalus, diffuse enlargement of the arachnoid spaces, diffuse villous hyperplasia of the choroid plexus and hypoplasia of the cerebellar vermis. (C) Axial T1-weighted MRI with contrast further highlights the diffusely enlarged choroid plexus within the lateral ventricles. (D) Sagital T1-weighted MRI without contrast demonstrates the hypoplastic cerebellar vermis consistent with Dandy-Walker malformation. (E) Intra-op composite endoscopic view of the right foramen of Monroe revealing the dense choroid plexus.

High-resolution array mapping of the child's genomic DNA demonstrated complete tetrasomy of the short arm of chromosome 9, establishing the karyotype of the child as 46XX+9p. Complete, non-mosaic tetrasomy 9p is an extremely rare, typically fatal syndrome with a broad range of clinical features ranging from normal phenotype to Dandy-Walker Malformation and perinatal demise. This is the first description of this genetic anomaly using high-resolution arrays, in a viable child broadening the clinical spectrum to include diffuse villous hyperplasia of the choroid plexus leading to hydrocephalus.

Clinical Presentation

The child presented to neurosurgical attention at the age of three months with an increasing head circumference, which crossed percentiles and failure to thrive. She was the product of a term pregnancy, born to healthy parents with no prior history of genetic disease. On examination, the head circumference was 42.5 cm. Sutures were splayed open and the anterior fontanelle was widened and tense. The child had a unilateral (left) cleft lip and palate, low-set ears, micrognathia, and beaking of the nose. Otherwise, there were no other noted systemic signs or symptoms. CT/MRI demonstrated ventriculomegaly, hyperplasia of the choroids plexus in the lateral ventricles, and a Dandy-Walker malformation variant.

Intervention/Technique

The patient was taken to the operating room and a ventriculoperitoneal shunt was placed under endoscopic guidance. Intra-op, marked hyperplasia of the choroid plexus was noted (Figure 1E). The CSF overproduction overwhelmed her abdominal absorptive capacity leading to CSF ascites and wound dehiscence. After an antibiotic course and shunt externalization (her CSF drainage was in excess of 1L/day), endoscopic-assisted surgical debulking of her bilateral choroid plexus hyperplasia was performed. The shunt was then successfully internalized. After two years of follow-up, her ventriculomegaly is gradually resolving as her shunt continues to function.

Copy Number Variant Analysis

Using the Beadstudio v3.3 genotyping software (Illumina, San Diego, CA, USA), analysis of the data revealed tetrasomy of the entire short arm of chromosome 9 (Figure 2). No other chromosomal anomalies were seen, indicating a karyotype/genotype of 46XX+

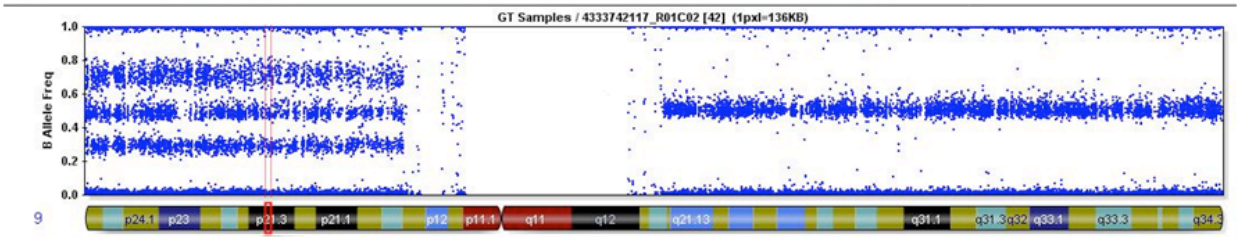

Figure 7: High-resolution SNP/CNV array analysis of the patient's genomic DNA. Tetrasomy of the short arm of chromosome 9: 46XX+9p (Illumina BeadStudio Chromosome 9 window, b-allele frequencies).

Cerebellar Atrophy and Pachygyria

Background

Non progressive human congenital ataxias are a rare, heterogeneous group of disorders that are characterized by motor disability, muscular hypotonia, incoordination, and impaired motor development.[95-97] They present initially with general symptoms such as delayed motor milestones and hypotonia during the post natal period and early childhood, followed by the gradual onset of ataxic gait during the first few years of life. Some cases improve as motor functions develop, while others worsen early during infancy as motor demands increase on coordination. [97]

This heterogeneous group of disorders has been associated with multiple other diseases including brain malformations, genetic syndromes, and congenital infections. It is thought that 4% of cases are due to a perinatal cause, while 45% of the cases are due to prenatal causes. The remaining half are speculated to be of unknown etiology.[96] Of the associated brain malformations, cerebellar hyoplasia seems to be the most common, occurring in slightly less than 50% of cases. [98] The most severe cases have been noted to have marked hyoplasia of the vermis ,and mild to moderate involvement of the neocerebellum, but in other cases the neuroimaging findings have not correlated with the severity of the disease.[98]

Evaluation of the distinguishable, inherited congenital ataxia syndromes with cerebellar hypoplasia has led to the identification of novel genes involved in the embryonic development of the cerebellum. Mutations in the *Reelin* gene have been identified to cause autosomal recessive lissencephaly with cerebellar hypoplasia [99], and *PTF1a* mutations have been linked to cerebellar agenesis and neonatal diabetes.[100] Studies on Joubert syndrome, a group of recessively inherited conditions characterized by congenital ataxia, hypotonia, episodic breathing, mental retardation, and a specific malformation of the brainstem, cerebellum, and peduncles, have led to the identification of several genes including *AHI1*, *NPHP1*, *CEP290*, *MKS3*, and *RPGR1L*; encoding cilia-like functioning and modular scaffolding proteins.[101-112]

Recently, mutations in the Very Low Density Lipoprotein Receptor (VLDLR) have been identified in patients in the Turkish [113 114], Iranian [115] and Hutterite [116] populations with

cerebellar atrophy and congenital ataxia following an autosomal recessive type of inheritance. These findings in conjunction with advances in the roles of these genes in mouse models have led to further understanding of the Relin-Vldlr pathway and its role in the developing cerebellum.

Clinical Presentation

The family originates from southeast Turkey. The two affected siblings are a product of a self-reported consanguineous first cousin marriage, ages 11 (NG 374-1) and 8 (NG 374-2) at the time of presentation (Figure 8). Both patients were delivered by uneventful c-sections with normal weights and heights at birth. They started holding their heads around 40 days, began to sit unsupported at age 1, and started walking at age 18 months with support from their hands. This is in contrast to unaffected children, which are able to walk unassisted on average by 15 months of age. The patients' gait is severely ataxic, and they demonstrate hyperactive deep tendon reflexes. They do not exhibit any tremor. Examination also reveals dysarthria, dysmetria, and dysdiadokinesis, and they cannot construct full sentences. The older patient exhibits selective mutism, constructing full sentences only when speaking to himself. MRI scans from both affected siblings show pachygyria and cerebellar atrophy (Figure 8).

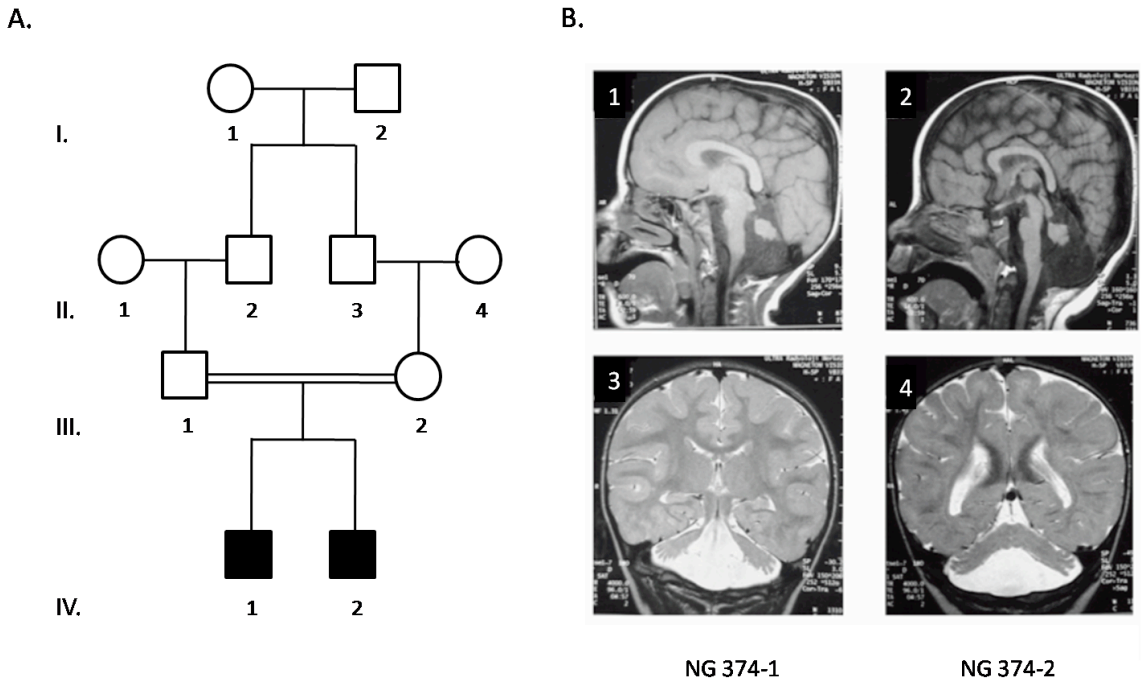

Figure 8

A. Representative pedigree of family NG-374. Affected members are identified by filled symbols. Diagonal lines indicate deceased family members. Circles represent female and squares represent male family members.

B. Magnetic Resonance Imaging (MRI) of the brain of affected siblings. Sagittal T1 (1,2) and Coronal T2 (3,4) weighted images demonstrate prominent pachygyria and hypoplasia of the cerebellar vermis and hemispheres in both patients NG 374-1 (1,3) and NG 374-2 (2,4).

Copy Number Variant Analysis

Homozygosity mapping of the affected siblings on Beadstudio v3.3 identified a 10 kb homozygous block shared by both patients in chromosome 9 starting at 102,542 bps and ending at 10,533,899 bps. Affected-only copy number variation analysis of both siblings on Human610-Quad beadchips using the PennCNV algorithm and visual inspection of the plotted intensities on Beadstudio v3.3 showed a shared homozygous deletion (Figure 9) on chromosome 9 spanning approximately 9.7 kb with the first and last deleted SNP markers being rs2375994 and rs10967306. The deletion was noted to be within the previously identified homozygous block on both patients. Compared to published reports of genomic variation in the Database of Human Variation (http://projects.tcag.ca/variation/), this area does not appear to be an area of common variability. Homozygous deletions in the *VLDLR* gene were absent in 300 other Turkish patients with malformations of cortical development that were genotyped.

PCR / QPCR Results

PCR analysis of the patients and parents revealed a homozygous deletion in the VLDRL gene encompassing exon 2, exon3, and exon 4 and no comparable homozygous deletion in the parents (Figure 9). Real time PCR analysis of the region confirmed the

homozygous deletion in both siblings, and also found a heterozygous deletion in both parents when compared to controls. (Figure 5) Sequence analysis revealed a 21,218 bp deletion including exons 2 ,3, and 4 and part of exons 1 and 5 that began on 2612144 bps and ends on 2633338 bps.

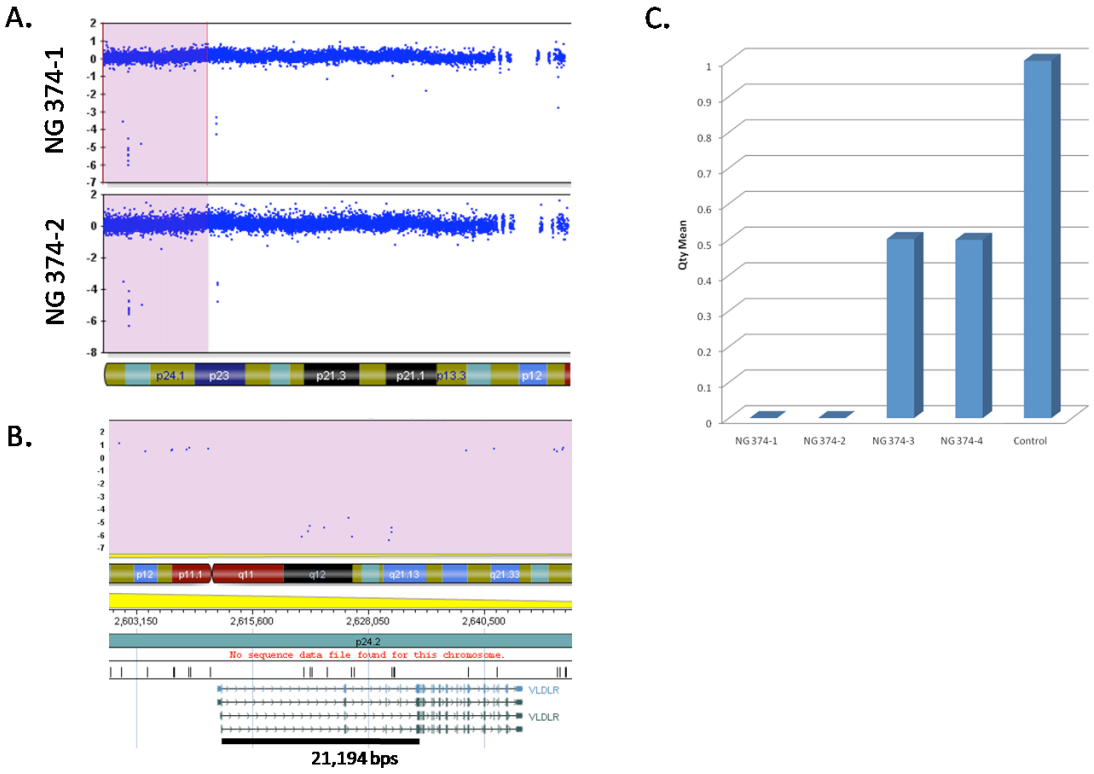

Figure 9:

A. Log R ratio plot of the genome-wide SNP based genotyping demonstrates a region on Chromosome 9 with a microdeletion in the VLDLR gene shared by both patients. Scatter points represent normalized log R ratios (y) for probe intensities along the chromosome. Negative values below y = -1 represent a homozygous deletion spanning 9 consecutive probes shared by both patients. Shaded areas represent areas of autozygosity.

B. Closer view of the deleted region on Chromosome 9 spanning 21,218 bps including the 9 consecutive SNPs. Deleted segment is represented by a black bar.

C. Quantitative PCR results of exon 3 of the *VLDLR* gene within the deleted segment showing homozygous deletions in both patients and heterozygous deletions in both parents.

Inbreeding Coefficient Estimates

Inbreeding coefficient estimates were obtained for each patient using the Inbreeding coefficient function of the Plink software. Because of the differences in the SNP marker densities, results were divided by beadchip type. The mean for the 127 patients genotyped on the Illumina Human CNV 370k was 0.034 with a range of -0.01 to 0.203. The mean for the 119 patients genotyped on the Illumina 610 Quad beadchip was 0.022 with a range of -0.014 to 0.175. The mean for the 40 controls genotyped on the Illumina 370k was 0.087 with a range of 0.015 to 0.22. The overall mean for all the 245 genotyped patients was 0.028 with a range of -0.012 to 0.203.

	370 Illumina Patients (n=127)	610 Illumina Patients (n=118)	Controls (n=40)
Range	-0.012 - 0.203	-0.014 – 0.176	0.015 - 0.22
Mean	0.034	0.022	0.087
Standard Deviation	0.042	0.039	0.041
Median	0.018	0.009	0.082
95%CI Mean	0.030 – 0.042	0.015-0.029	0.082 - 0.093

Table 7: Inbreeding coefficients for each subgroup. Inbreeding coefficients were compared between patients that had self reported consanguinity versus patients with unknown or reported no consanguinity. The mean of the inbreeding coefficients for patients that were reported as consanguineous was 0.075 while the mean of the patients reported as non consanguineous or unknown was 0.005

	Reported As Cons	Reported As Non-Cons
Range	-0.007 - 0.22	-0.01 - 0.038
Mean	0.075	0.005
Standard Deviation	0.045	0.010
Median	0.072	0.002
95%CI Mean	0.07 - 0.08	0.004 - 0.007

Table 8: Inbreeding coefficients for patients reported as consanguineous and patients reported as non-consanguineous. Inbreeding coefficient mean for patients reported as consanguineous was significantly higher than the inbreeding coefficient for patients reported as non-consanguineous.

Homozygosity Mapping

We are currently in the process of performing homozygosity mapping on our samples (results not shown) in order to find common homozygous areas that may harbor homozygous mutations responsible for autosomal recessive diseases in the consanguineous cohort. Inbreeding coefficients will be used to select a consanguineous group of patients.

DISCUSSION

The results of the two studies presented above demonstrate the utility of SNP genotyping and CNV analysis in uncovering the genetic basis of malformations of cortical development. Specifically, two diseases are presented in this manuscript: choroid hyperplasia, and cerebellar atrophy as part of the ongoing effort to identify disease-causing mutations in our cohort of patients with cortical malformations.

Choroid Hyperplasia

First described in 1973[117], tetrasomy 9p as a rare congenital chromosomal anomaly. Since that time, approximately 50 cases have been reported with a wide variety of phenotypic variants. The severity of phenotype appears to correlate with the degree of mosaicism with non-mosaic cases resulting in perinatal demise in the first few weeks of life[118-123]. The majority of cases of 9p tetrasomy are mosaic and thus accounting for the diverse range of mild to severe phenotypes. Commonality among the phenotypes has allowed for a syndrome to emerge consisting of hypertelorism, beaked nose, cleft palate and midface abnormalities, ear malformations, skeletal and joint abnormalities, hypoplasia of the nails and digits, hypertelorism, urogenital anomalies, developmental retardation, hypotonia, open sutures/wide fontanelles, clinodactyly, growth retardation, and ventriculomegaly/macrocephaly or microcephaly[119, 120, 124, 125].

Three prior infants have been described with choroid plexus pathology in association with 9p duplications. Norman et al reported two patients, one with hemorrhagic choroid plexus hyperplasia, early perinatal demise, and mosaic tetrasomy of 9p karyotype of 47,XY,+idic(9)(q11) and a second child developed hydrocephalus at 11 months with choroid plexus hyperplasia on ultrasound and a trisomy 9p karyotype of 47, XX, +der(9)t(9;?)(q13;?)[126]. The unknown, precise definition of the duplication demonstrates the low-resolution of Giemsa banding and traditional FISH analysis. Shapiro et al described a patient with bilateral choroid plexus "papillomata" and partial 9p tetrasomy, partial 9p trisomy and a karyotype of 47, XX,+psudic(9)t(9;9)(9pter→9q22.1::9q12 or 13→9pter)[123]. Hydrocephalus was initially thought to be a feature not seen in non-mosaic 9p duplications[125], however, numerous children are reported with mosaic and non-mosaic 9p duplications (trisomy or tetrasomy, complete or partial) associated with hydrocephalus[119, 120, 122, 125, 127-130] or hydrocephalus specifically from Dandy-Walker malformations[118, 131-139]. Only previously mentioned two papers specifically discuss the presence of choroid plexus abnormalities[123, 126].

DVHCP is a rare disorder and results from treatment are limited to those reported in fewer than 10 reported cases. Two reports have demonstrated complete resolution of hydrocephalus after choroid plexus resection, however there was associated morbidity with the approach[140, 141]. The majority of cases argue for debulking of the choroid plexus and subsequent shunting as externalized ventricular drainage failed to demonstrate complete cessation of CSF overproduction[90-94, 142]. This was the approach employed by our group.

The presence of 9p duplications has been examined in choroid plexus tumor specimens: cytogenic studies on 49 choroid plexus tumors found 9p duplication in 50% of choroid plexus papillomas and 33% of choroid plexus carcinomas[143], while others have not been able to demonstrate consistent 9p duplications in choroid plexus tumors[126, 144]. The gain of 9p was associated with a significantly longer survival, and better prognosis for patients with choroid carcinomas[143]. There likely exist genes on 9p, which play a role in choroid plexus growth and development. This report expands the spectrum of phenotypic anomalies associated with non-mosaic tetrasomy 9p syndrome to include DVHCP. As we refine the intervals on chromosome 9p involved, we will understand the relation of genes on 9p to midline anomalies and the growth and tumorigenesis of the choroid plexus.

Cerebellar Atrophy

The *VLDLR* gene is composed of 19 exons, spans 32 kb, and encodes a protein that is part of the Low Density Lipoprotein (LDL) gene family. It encodes a five domain, ligand binding receptor that is characterized by an N terminal 328-amino acid cysteine-rich ligand-binding domain, a 396-amino acid EGF precursor homology domain, a 46-amino acid O-linked sugar domain, a 22-amino acid single transmembrane domain, and a 54-amino acid cytoplasmic COOH terminal domain. In humans two forms of the receptor have been identified, one that resembles the LDL receptor, and an alternative form with four domains that lacks the O-linked sugar domain. [145].The VLDLR has been suggested to be important in the metabolism of apoprotein-E containing triacylglycerol-rich

lipoproteins, beta-migrating VLDL and intermediate-density lipoproteins.[146] It is also part of the Reelin signaling pathway [147].

Reelin is an extracellular glycoprotein that is secreted by several types of neurons, including the Cajal-Retzius cells in the marginal zones of the cortex during embryonic development.[148] It is important in the regulation of neuronal migration and positioning in the developing brain, as well as modulating synaptic plasticity and long term potentiation in the hippocampus during adulthood[149]. It has also been shown to stimulate dendrite and dentritic spine development [150], and the continual migration of neuroblasts generated in adult neurogenesis sites such as the subventricular zone and dentate nucleus.[151] It is thought to interact through one of two receptors, the VLDLR and the Apolipoprotein-E Receptor Type 2 (ApoER2)[152], on several intracellular proteins including Dab-1, an adapter protein. [147] According to a recent study, these two receptors might have divergent roles with VLDLR conducting the stop signal for migrating neurons while ApoER2 is essential for the migration of late-born neocortical neurons.[153]

Reelin -/- mice were originally described by Falconer et. al in 1951 and were named for their distinct ataxic and "reeling" gait.[154] Affected mice exhibit failed migration of the Purkinje cells, inverted cortical lamination, cerebellar hypoplasia, and ataxia.[155-158]. In humans, homozygous mutations of the Reelin gene are responsible for a type of autosomal recessive lissencephally, Norman-Roberts syndrome[99]. Another protein found to have a role in lissencephally, Pafahb1 (LIS1), was also shown to be part of the reelin pathway, interacting with the intracellular segment of VLDLR.[159]

Mutations in the *VLDRL* gene have been previously described both in humans and in animal models. *Vldlr* $^{-/-}$ mice appear to be grossly and neurologically normal, but contain ectopically located Purkinje cells in the cerebellum and radially aligned neurons in the cortex that appear to have failed to distribute[152, 160]. The first mutation observed in a human case in the gene was in the Hutterite population[116] where a 199-kb homozygous deletion encompassing the complete VLDLR gene and possibly adjacent regulatory regions was noted to be responsible for the "Dysequillibrium Syndrome". Originally described in the 1980s, the "Dysequillibrium Syndrome" in the Hutterite population consisted of an autosomal recessive constellation of non-progressive cerebellar ataxia, mental retardation, and cerebellar hypoplasia[161, 162]. Patients were also noted to have delayed ambulation, strabismus, mild cortical simplification on MRI, and short stature (15%). However, this deletion also encompassed adjacent regulatory regions, and possibly a second gene. It was therefore unclear whether a mutation in *VLDRL* could solely explain the syndrome in its entirety. Subsequently, a homozygous nucleotide substitution in exon 10 resulting in a premature stop codon in the *VLDLR* gene identified in an Iranian family with Disequilibrium Syndrome gave rest to this argument, and indeed showed that a truncated VLDRL protein in isolation was a satisfactory cause of DES.

Since then, three Turkish families have been reported with Unertan Syndrome, which is a rare autosomal recessive neurodevelopmental condition with cerebellar and cortical hypoplasia accompanied by mental retardation, primitive and dysarthric speech, and most

notably, quadrupedal locomotion[163]. One non-sense and one frameshift mutation (in two separate families) resulting in premature stop codons in exons 5 and 17 were identified in the Turkish families with Unertan syndrome, presumably causing the *VLDLR* to lack transmembrane and signaling domains.

The cause of differences in locomotion phenotype are unclear, but Ozcelik et al. argue that it might be a result of different mutations in the same gene leading to different phenotypes, and variable expressions of the disease phenotype.[114, 164] Ozcelik et al explain that they believe quadrupedal gait to be the result of their reported homozygous deletions resulting in this specific gait compared to the mutations resulting in the Dysequillibrium syndrome. In contrast, Herz and Humphrey argue that quadrupedal locomotion has developed in a subset of reported patients with *VLDLR* deletions as an adaptive process to the severe truncal ataxia, and the Unertan syndrome does not represent a separate genetic entity[165, 166]. They believe that rural surfaces, imitation of the behavior of other affected siblings, lack of medical attention, and social acceptance of quadrupedal gait without correction are believed to have contributed to the development of quadrupedal gait in these patients. Even though it is true that some families were isolated from medical attention, this claim has also been debated by the presence of families where extensive medical care was sought, and quadrupedal gait was strongly discouraged yet still developed.

Including our recent report, to date five different mutations in nine families have been described in the *VLDLR* gene including the original description in the Hutterites.

Structural examination of the gene and the defective protein does not reveal any identifiable portion that seems to be responsible for quadrupedal gait. A stop codon in exon 5 and a frameshift mutation in exon 17 both lead to quadrupedal gait in Turkish families, whereas a stop codon in exon 10, and our recent report of a deletion affecting exons 1-5 resulted in bipedal, ataxic gait. Thus, it is likely that DES and Unertan syndrome are clinically, but not genetically distinct syndromes, and represent a spectrum of disease resulting from dysfunctional VLDLR protein. Where along the spectrum an affected patient will lay is likely the product of a complex interaction between genetic makeup and the environment, and cannot be predicted based on the mutation alone. It is unlikely that *VLDRL* represents an indispensable gene in human bipedalism and evolution, but rather an integral part of cerebellogenesis.

REFERENCES

1. Pang, T., Atefy, R. & Sheen, V. Malformations of cortical development. *Neurologist* **14**, 181-91 (2008).
2. Kuzniecky, R.I. Magnetic resonance imaging in developmental disorders of the cerebral cortex. *Epilepsia* **35 Suppl 6**, S44-56 (1994).
3. Barkovich, A.J., Kuzniecky, R.I., Jackson, G.D., Guerrini, R. & Dobyns, W.B. A developmental and genetic classification for malformations of cortical development. *Neurology* **65**, 1873-87 (2005).
4. Lombroso, C.T. Can early postnatal closed head injury induce cortical dysplasia. *Epilepsia* **41**, 245-53 (2000).
5. Sarnat, H.B. Disturbances of late neuronal migrations in the perinatal period. *Am J Dis Child* **141**, 969-80 (1987).
6. Kumar, D. Disorders of the genome architecture: a review. *Genomic Med* (2009).
7. Jackson, A.P. et al. Identification of microcephalin, a protein implicated in determining the size of the human brain. *Am J Hum Genet* **71**, 136-42 (2002).
8. Bond, J. et al. ASPM is a major determinant of cerebral cortical size. *Nat Genet* **32**, 316-20 (2002).
9. Bond, J. et al. Protein-truncating mutations in ASPM cause variable reduction in brain size. *Am J Hum Genet* **73**, 1170-7 (2003).
10. Bond, J. et al. A centrosomal mechanism involving CDK5RAP2 and CENPJ controls brain size. *Nat Genet* **37**, 353-5 (2005).
11. Zhong, X., Pfeifer, G.P. & Xu, X. Microcephalin encodes a centrosomal protein. *Cell Cycle* **5**, 457-8 (2006).
12. Zhong, X., Liu, L., Zhao, A., Pfeifer, G.P. & Xu, X. The abnormal spindle-like, microcephaly-associated (ASPM) gene encodes a centrosomal protein. *Cell Cycle* **4**, 1227-9 (2005).
13. do Carmo Avides, M. & Glover, D.M. Abnormal spindle protein, Asp, and the integrity of mitotic centrosomal microtubule organizing centers. *Science* **283**, 1733-5 (1999).
14. Fox, J.W. et al. Mutations in filamin 1 prevent migration of cerebral cortical neurons in human periventricular heterotopia. *Neuron* **21**, 1315-25 (1998).
15. Sheen, V.L. et al. Mutations in the X-linked filamin 1 gene cause periventricular nodular heterotopia in males as well as in females. *Hum Mol Genet* **10**, 1775-83 (2001).
16. Moro, F. et al. Familial periventricular heterotopia: missense and distal truncating mutations of the FLN1 gene. *Neurology* **58**, 916-21 (2002).
17. Sheen, V.L. et al. Etiological heterogeneity of familial periventricular heterotopia and hydrocephalus. *Brain Dev* **26**, 326-34 (2004).
18. des Portes, V. et al. doublecortin is the major gene causing X-linked subcortical laminar heterotopia (SCLH). *Hum Mol Genet* **7**, 1063-70 (1998).
19. Reiner, O. et al. Isolation of a Miller-Dieker lissencephaly gene containing G protein beta-subunit-like repeats. *Nature* **364**, 717-21 (1993).

20. Gleeson, J.G. et al. Doublecortin, a brain-specific gene mutated in human X-linked lissencephaly and double cortex syndrome, encodes a putative signaling protein. *Cell* **92**, 63-72 (1998).
21. Poirier, K. et al. Large spectrum of lissencephaly and pachygyria phenotypes resulting from de novo missense mutations in tubulin alpha 1A (TUBA1A). *Hum Mutat* **28**, 1055-64 (2007).
22. Keays, D.A. et al. Mutations in alpha-tubulin cause abnormal neuronal migration in mice and lissencephaly in humans. *Cell* **128**, 45-57 (2007).
23. Bonneau, D. et al. X-linked lissencephaly with absent corpus callosum and ambiguous genitalia (XLAG): clinical, magnetic resonance imaging, and neuropathological findings. *Ann Neurol* **51**, 340-9 (2002).
24. Beltran-Valero de Bernabe, D. et al. Mutations in the O-mannosyltransferase gene POMT1 give rise to the severe neuronal migration disorder Walker-Warburg syndrome. *Am J Hum Genet* **71**, 1033-43 (2002).
25. van Reeuwijk, J. et al. POMT2 mutations cause alpha-dystroglycan hypoglycosylation and Walker-Warburg syndrome. *J Med Genet* **42**, 907-12 (2005).
26. Yoshida, A. et al. Muscular dystrophy and neuronal migration disorder caused by mutations in a glycosyltransferase, POMGnT1. *Dev Cell* **1**, 717-24 (2001).
27. Toda, T. et al. Refined mapping of a gene responsible for Fukuyama-type congenital muscular dystrophy: evidence for strong linkage disequilibrium. *Am J Hum Genet* **55**, 946-50 (1994).
28. Piao, X. et al. An autosomal recessive form of bilateral frontoparietal polymicrogyria maps to chromosome 16q12.2-21. *Am J Hum Genet* **70**, 1028-33 (2002).
29. Piao, X. et al. Genotype-phenotype analysis of human frontoparietal polymicrogyria syndromes. *Ann Neurol* **58**, 680-7 (2005).
30. Lupski, J.R. Genomic disorders: structural features of the genome can lead to DNA rearrangements and human disease traits. *Trends Genet* **14**, 417-22 (1998).
31. Pentao, L., Wise, C.A., Chinault, A.C., Patel, P.I. & Lupski, J.R. Charcot-Marie-Tooth type 1A duplication appears to arise from recombination at repeat sequences flanking the 1.5 Mb monomer unit. *Nat Genet* **2**, 292-300 (1992).
32. Reiter, L.T. et al. A recombination hotspot responsible for two inherited peripheral neuropathies is located near a mariner transposon-like element. *Nat Genet* **12**, 288-97 (1996).
33. Edelmann, L., Pandita, R.K. & Morrow, B.E. Low-copy repeats mediate the common 3-Mb deletion in patients with velo-cardio-facial syndrome. *Am J Hum Genet* **64**, 1076-86 (1999).
34. Amos-Landgraf, J.M. et al. Chromosome breakage in the Prader-Willi and Angelman syndromes involves recombination between large, transcribed repeats at proximal and distal breakpoints. *Am J Hum Genet* **65**, 370-86 (1999).
35. Cheung, V.G. et al. Integration of cytogenetic landmarks into the draft sequence of the human genome. *Nature* **409**, 953-8 (2001).
36. Cheung, J. et al. Genome-wide detection of segmental duplications and potential assembly errors in the human genome sequence. *Genome Biol* **4**, R25 (2003).

37. She, X. et al. Shotgun sequence assembly and recent segmental duplications within the human genome. *Nature* **431**, 927-30 (2004).
38. Britten, R.J. & Davidson, E.H. Studies on nucleic acid reassociation kinetics: empirical equations describing DNA reassociation. *Proc Natl Acad Sci U S A* **73**, 415-9 (1976).
39. Eichler, E.E., Archidiacono, N. & Rocchi, M. CAGGG repeats and the pericentromeric duplication of the hominoid genome. *Genome Res* **9**, 1048-58 (1999).
40. Shaw, C.J. & Lupski, J.R. Implications of human genome architecture for rearrangement-based disorders: the genomic basis of disease. *Hum Mol Genet* **13 Spec No 1**, R57-64 (2004).
41. Lupski, J.R. & Stankiewicz, P. Genomic disorders: molecular mechanisms for rearrangements and conveyed phenotypes. *PLoS Genet* **1**, e49 (2005).
42. Somerville, M.J. et al. Severe expressive-language delay related to duplication of the Williams-Beuren locus. *N Engl J Med* **353**, 1694-701 (2005).
43. Bittel, D.C. & Butler, M.G. Prader-Willi syndrome: clinical genetics, cytogenetics and molecular biology. *Expert Rev Mol Med* **7**, 1-20 (2005).
44. Long, F.L., Duckett, D.P., Billam, L.J., Williams, D.K. & Crolla, J.A. Triplication of 15q11-q13 with inv dup(15) in a female with developmental delay. *J Med Genet* **35**, 425-8 (1998).
45. Potocki, L. et al. Molecular mechanism for duplication 17p11.2- the homologous recombination reciprocal of the Smith-Magenis microdeletion. *Nat Genet* **24**, 84-7 (2000).
46. Edelmann, L. et al. A common molecular basis for rearrangement disorders on chromosome 22q11. *Hum Mol Genet* **8**, 1157-67 (1999).
47. De Luca, A. et al. Deletions of NF1 gene and exons detected by multiplex ligation-dependent probe amplification. *J Med Genet* **44**, 800-8 (2007).
48. Bailey, J.A. & Eichler, E.E. Primate segmental duplications: crucibles of evolution, diversity and disease. *Nat Rev Genet* **7**, 552-64 (2006).
49. Gu, W., Zhang, F. & Lupski, J.R. Mechanisms for human genomic rearrangements. *Pathogenetics* **1**, 4 (2008).
50. Bayrakli, F. et al. Rapid identification of disease-causing mutations using copy number analysis within linkage intervals. *Hum Mutat* **28**, 1236-40 (2007).
51. Kitada, T. et al. Mutations in the parkin gene cause autosomal recessive juvenile parkinsonism. *Nature* **392**, 605-8 (1998).
52. Lupski, J.R. Genomic rearrangements and sporadic disease. *Nat Genet* **39**, S43-7 (2007).
53. Kalter, H., Ormsby, I. & Warkany, J. Congenital malformations of the central nervous system and transplacental carcinogenesis: modification of ethylnitrosourea-induced brain tumors in rats by pretreatment with methylazoxymethanol. *Int J Biol Res Pregnancy* **3**, 93-8 (1982).
54. Kalter, H. & Warkany, J. Congenital malformations (second of two parts). *N Engl J Med* **308**, 491-7 (1983).
55. Baird, P.A., Anderson, T.W., Newcombe, H.B. & Lowry, R.B. Genetic disorders in children and young adults: a population study. *Am J Hum Genet* **42**, 677-93 (1988).

56. Kondrashov, A.S. Direct estimates of human per nucleotide mutation rates at 20 loci causing Mendelian diseases. *Hum Mutat* **21**, 12-27 (2003).
57. Crow, J.F. Age and sex effects on human mutation rates: an old problem with new complexities. *J Radiat Res (Tokyo)* **47 Suppl B**, B75-82 (2006).
58. Crow, J.F. The origins, patterns and implications of human spontaneous mutation. *Nat Rev Genet* **1**, 40-7 (2000).
59. Stankiewicz, P. & Lupski, J.R. Genome architecture, rearrangements and genomic disorders. *Trends Genet* **18**, 74-82 (2002).
60. Lieber, M.R., Ma, Y., Pannicke, U. & Schwarz, K. Mechanism and regulation of human non-homologous DNA end-joining. *Nat Rev Mol Cell Biol* **4**, 712-20 (2003).
61. Lieber, M.R., Lu, H., Gu, J. & Schwarz, K. Flexibility in the order of action and in the enzymology of the nuclease, polymerases, and ligase of vertebrate non-homologous DNA end joining: relevance to cancer, aging, and the immune system. *Cell Res* **18**, 125-33 (2008).
62. Nobile, C. et al. Analysis of 22 deletion breakpoints in dystrophin intron 49. *Hum Genet* **110**, 418-21 (2002).
63. Toffolatti, L. et al. Investigating the mechanism of chromosomal deletion: characterization of 39 deletion breakpoints in introns 47 and 48 of the human dystrophin gene. *Genomics* **80**, 523-30 (2002).
64. Lee, J.A., Carvalho, C.M. & Lupski, J.R. A DNA replication mechanism for generating nonrecurrent rearrangements associated with genomic disorders. *Cell* **131**, 1235-47 (2007).
65. Slack, A., Thornton, P.C., Magner, D.B., Rosenberg, S.M. & Hastings, P.J. On the mechanism of gene amplification induced under stress in Escherichia coli. *PLoS Genet* **2**, e48 (2006).
66. Lupski, J.R. et al. DNA duplication associated with Charcot-Marie-Tooth disease type 1A. *Cell* **66**, 219-32 (1991).
67. Lupski, J.R. et al. Gene dosage is a mechanism for Charcot-Marie-Tooth disease type 1A. *Nat Genet* **1**, 29-33 (1992).
68. Lee, J.A. et al. Role of genomic architecture in PLP1 duplication causing Pelizaeus-Merzbacher disease. *Hum Mol Genet* **15**, 2250-65 (2006).
69. Kriek, M. et al. Copy number variation in regions flanked (or unflanked) by duplicons among patients with developmental delay and/or congenital malformations; detection of reciprocal and partial Williams-Beuren duplications. *Eur J Hum Genet* **14**, 180-9 (2006).
70. Berg, J.S. et al. Speech delay and autism spectrum behaviors are frequently associated with duplication of the 7q11.23 Williams-Beuren syndrome region. *Genet Med* **9**, 427-41 (2007).
71. Padiath, Q.S. et al. Lamin B1 duplications cause autosomal dominant leukodystrophy. *Nat Genet* **38**, 1114-23 (2006).
72. Mei, D. et al. High frequency of genomic deletions--and a duplication--in the LIS1 gene in lissencephaly: implications for molecular diagnosis. *J Med Genet* **45**, 355-61 (2008).
73. Bi, W. et al. Increased LIS1 expression affects human and mouse brain development. *Nat Genet* **41**, 168-77 (2009).

74. Koolen, D.A. et al. A new chromosome 17q21.31 microdeletion syndrome associated with a common inversion polymorphism. *Nat Genet* **38**, 999-1001 (2006).
75. Varela, M.C. et al. A 17q21.31 microdeletion encompassing the MAPT gene in a mentally impaired patient. *Cytogenet Genome Res* **114**, 89-92 (2006).
76. Sharp, A.J. et al. A recurrent 15q13.3 microdeletion syndrome associated with mental retardation and seizures. *Nat Genet* **40**, 322-8 (2008).
77. Altshuler, D., Daly, M.J. & Lander, E.S. Genetic mapping in human disease. *Science* **322**, 881-8 (2008).
78. Kruglyak, L. & Nickerson, D.A. Variation is the spice of life. *Nat Genet* **27**, 234-6 (2001).
79. The International HapMap Project. *Nature* **426**, 789-96 (2003).
80. Frazer, K.A. et al. A second generation human haplotype map of over 3.1 million SNPs. *Nature* **449**, 851-61 (2007).
81. Feuk, L., Carson, A.R. & Scherer, S.W. Structural variation in the human genome. *Nat Rev Genet* **7**, 85-97 (2006).
82. Sebat, J. et al. Large-scale copy number polymorphism in the human genome. *Science* **305**, 525-8 (2004).
83. Iafrate, A.J. et al. Detection of large-scale variation in the human genome. *Nat Genet* **36**, 949-51 (2004).
84. Freeman, J.L. et al. Copy number variation: new insights in genome diversity. *Genome Res* **16**, 949-61 (2006).
85. Wirtenberger, M., Hemminki, K. & Burwinkel, B. Identification of frequent chromosome copy-number polymorphisms by use of high-resolution single-nucleotide-polymorphism arrays. *Am J Hum Genet* **78**, 520-2 (2006).
86. Bell, G.I., Karam, J.H. & Rutter, W.J. Polymorphic DNA region adjacent to the 5' end of the human insulin gene. *Proc Natl Acad Sci U S A* **78**, 5759-63 (1981).
87. Wang, K. et al. PennCNV: an integrated hidden Markov model designed for high-resolution copy number variation detection in whole-genome SNP genotyping data. *Genome Res* **17**, 1665-74 (2007).
88. Jakobsson, M. et al. Genotype, haplotype and copy-number variation in worldwide human populations. *Nature* **451**, 998-1003 (2008).
89. Purcell, S. et al. PLINK: a tool set for whole-genome association and population-based linkage analyses. *Am J Hum Genet* **81**, 559-75 (2007).
90. Aziz, A.A., Coleman, L., Morokoff, A. & Maixner, W. Diffuse choroid plexus hyperplasia: an under-diagnosed cause of hydrocephalus in children? *Pediatr Radiol* **35**, 815-8 (2005).
91. Britz, G.W., Kim, D.K. & Loeser, J.D. Hydrocephalus secondary to diffuse villous hyperplasia of the choroid plexus. Case report and review of the literature. *J Neurosurg* **85**, 689-91 (1996).
92. Fujimoto, Y., Matsushita, H., Plese, J.P. & Marino, R., Jr. Hydrocephalus due to diffuse villous hyperplasia of the choroid plexus. Case report and review of the literature. *Pediatr Neurosurg* **40**, 32-6 (2004).
93. Iplikcioglu, A.C., Bek, S., Gokduman, C.A., Bikmaz, K. & Cosar, M. Diffuse villous hyperplasia of choroid plexus. *Acta Neurochir (Wien)* **148**, 691-4; discussion 694 (2006).

94. Smith, Z.A. et al. Choroid plexus hyperplasia: surgical treatment and immunohistochemical results. Case report. *J Neurosurg* **107**, 255-62 (2007).
95. Sanner, G. & Hagberg, B. 188 cases of non-progressive ataxic syndromes in childhood. Aspects of aetiology and classification. *Neuropadiatrie* **5**, 224-35 (1974).
96. Esscher, E., Flodmark, O., Hagberg, G. & Hagberg, B. Non-progressive ataxia: origins, brain pathology and impairments in 78 swedish children. *Dev Med Child Neurol* **38**, 285-96 (1996).
97. Steinlin, M. Non-progressive congenital ataxias. *Brain Dev* **20**, 199-208 (1998).
98. Steinlin, M., Zangger, B. & Boltshauser, E. Non-progressive congenital ataxia with or without cerebellar hypoplasia: a review of 34 subjects. *Dev Med Child Neurol* **40**, 148-54 (1998).
99. Hong, S.E. et al. Autosomal recessive lissencephaly with cerebellar hypoplasia is associated with human RELN mutations. *Nat Genet* **26**, 93-6 (2000).
100. Sellick, G.S. et al. Mutations in PTF1A cause pancreatic and cerebellar agenesis. *Nat Genet* **36**, 1301-5 (2004).
101. Joubert, M., Eisenring, J.J., Robb, J.P. & Andermann, F. Familial agenesis of the cerebellar vermis. A syndrome of episodic hyperpnea, abnormal eye movements, ataxia, and retardation. *Neurology* **19**, 813-25 (1969).
102. Dixon-Salazar, T. et al. Mutations in the AHI1 gene, encoding jouberin, cause Joubert syndrome with cortical polymicrogyria. *Am J Hum Genet* **75**, 979-87 (2004).
103. Ferland, R.J. et al. Abnormal cerebellar development and axonal decussation due to mutations in AHI1 in Joubert syndrome. *Nat Genet* **36**, 1008-13 (2004).
104. Castori, M. et al. NPHP1 gene deletion is a rare cause of Joubert syndrome related disorders. *J Med Genet* **42**, e9 (2005).
105. Parisi, M.A. et al. The NPHP1 gene deletion associated with juvenile nephronophthisis is present in a subset of individuals with Joubert syndrome. *Am J Hum Genet* **75**, 82-91 (2004).
106. Valente, E.M. et al. Mutations in CEP290, which encodes a centrosomal protein, cause pleiotropic forms of Joubert syndrome. *Nat Genet* **38**, 623-5 (2006).
107. Baala, L. et al. The Meckel-Gruber syndrome gene, MKS3, is mutated in Joubert syndrome. *Am J Hum Genet* **80**, 186-94 (2007).
108. Brancati, F. et al. MKS3/TMEM67 mutations are a major cause of COACH Syndrome, a Joubert Syndrome related disorder with liver involvement. *Hum Mutat* **30**, E432-E442 (2008).
109. Arts, H.H. et al. Mutations in the gene encoding the basal body protein RPGRIP1L, a nephrocystin-4 interactor, cause Joubert syndrome. *Nat Genet* **39**, 882-8 (2007).
110. Brancati, F. et al. RPGRIP1L mutations are mainly associated with the cerebello-renal phenotype of Joubert syndrome-related disorders. *Clin Genet* **74**, 164-70 (2008).
111. Delous, M. et al. The ciliary gene RPGRIP1L is mutated in cerebello-oculo-renal syndrome (Joubert syndrome type B) and Meckel syndrome. *Nat Genet* **39**, 875-81 (2007).

112. Wolf, M.T. et al. Mutational analysis of the RPGRIP1L gene in patients with Joubert syndrome and nephronophthisis. *Kidney Int* **72**, 1520-6 (2007).
113. Turkmen, S. et al. Cerebellar hypoplasia, with quadrupedal locomotion, caused by mutations in the very low-density lipoprotein receptor gene. *Eur J Hum Genet* **16**, 1070-4 (2008).
114. Ozcelik, T. et al. Mutations in the very low-density lipoprotein receptor VLDLR cause cerebellar hypoplasia and quadrupedal locomotion in humans. *Proc Natl Acad Sci U S A* **105**, 4232-6 (2008).
115. Moheb, L.A. et al. Identification of a nonsense mutation in the very low-density lipoprotein receptor gene (VLDLR) in an Iranian family with dysequilibrium syndrome. *Eur J Hum Genet* **16**, 270-3 (2008).
116. Boycott, K.M. et al. Homozygous deletion of the very low density lipoprotein receptor gene causes autosomal recessive cerebellar hypoplasia with cerebral gyral simplification. *Am J Hum Genet* **77**, 477-83 (2005).
117. Ghymers, D., Hermann, B., Disteche, C. & Frederic, J. [Partial tetrasomy of number 9 chromosome, and mosaicism in a child with multiple malformations (author's transl)]. *Humangenetik* **20**, 273-82 (1973).
118. di Vera, E. et al. Rhombencephalosynapsis in a severely polymalformed fetus with non-mosaic tetrasomy 9p, in intracytoplasmic-sperm-injection pregnancy. *J Assist Reprod Genet* **25**, 577-80 (2008).
119. de Azevedo Moreira, L.M., Freitas, L.M., Gusmao, F.A. & Riegel, M. New case of non-mosaic tetrasomy 9p in a severely polymalformed newborn girl. *Birth Defects Res A Clin Mol Teratol* **67**, 985-8 (2003).
120. Tonk, V.S. Moving towards a syndrome: a review of 20 cases and a new case of non-mosaic tetrasomy 9p with long-term survival. *Clin Genet* **52**, 23-9 (1997).
121. Leichtman, L.G., Zackowski, J.L., Storto, P.D. & Newlin, A. Non-mosaic tetrasomy 9p in a liveborn infant with multiple congenital anomalies: case report and comparison with trisomy 9p. *Am J Med Genet* **63**, 434-7 (1996).
122. Jalal, S.M., Kukolich, M.K., Garcia, M., Benjamin, T.R. & Day, D.W. Tetrasomy 9p: an emerging syndrome. *Clin Genet* **39**, 60-4 (1991).
123. Shapiro, S.D., Hansen, K.L. & Littlefield, C.A. Brief clinical report: non-mosaic partial tetrasomy and partial trisomy 9. *Am J Med Genet* **20**, 271-6 (1985).
124. Dhandha, S., Hogge, W.A., Surti, U. & McPherson, E. Three cases of tetrasomy 9p. *Am J Med Genet* **113**, 375-80 (2002).
125. Schaefer, G.B., Domek, D.B., Morgan, M.A., Muneer, R.S. & Johnson, S.F. Tetrasomy of the short arm of chromosome 9: prenatal diagnosis and further delineation of the phenotype. *Am J Med Genet* **38**, 612-5 (1991).
126. Norman, M.G., Harrison, K.J., Poskitt, K.J. & Kalousek, D.K. Duplication of 9P and hyperplasia of the choroid plexus: a pathologic, radiologic, and molecular cytogenetics study. *Pediatr Pathol Lab Med* **15**, 109-20 (1995).
127. Cavalcanti, D.P., Ferrari, I., de Almeida, J.C., de Pina Neto, J.M. & de Oliveira, J.A. Tetrasomy 9p caused by idic (9) (pter----q13----pter). *Am J Med Genet* **27**, 497-503 (1987).
128. Rutten, F.J., Scheres, J.M., Hustinx, T.W. & ter Haar, B.G. A presumptive tetrasomy for the short arm of chromosome 9. *Humangenetik* **25**, 163-70 (1974).

129. Cuoco, C. et al. Duplication of the short arm of chromosome 9. Analysis of five cases. *Hum Genet* **61**, 3-7 (1982).
130. Garcia-Cruz, D. et al. Tetrasomy 9p: clinical aspects and enzymatic gene dosage expression. *Ann Genet* **25**, 237-42 (1982).
131. Cazorla Calleja, M.R., Verdu, A. & Felix, V. Dandy-Walker malformation in an infant with tetrasomy 9p. *Brain Dev* **25**, 220-3 (2003).
132. Chen, C.P. et al. Prenatal diagnosis of the Dandy-Walker malformation and ventriculomegaly associated with partial trisomy 9p and distal 12p deletion. *Prenat Diagn* **22**, 1063-6 (2002).
133. Chen, C.P., Chen, C.P. & Shih, J.C. Association of partial trisomy 9p and the Dandy-Walker malformation. *Am J Med Genet A* **132A**, 111-2 (2005).
134. Deurloo, K.L. et al. Prenatal diagnosis of tetrasomy 9p in a 19-week-old fetus with Dandy-Walker malformation: a case report. *Prenat Diagn* **24**, 796-8 (2004).
135. Hannam, S., Greenough, A. & Dawson, J.M. An unusual presentation of trisomy 9p syndrome with a partial Dandy-Walker malformation. *Eur J Pediatr* **158**, 1012 (1999).
136. Hengstschlager, M. et al. Prenatal diagnosis of tetrasomy 9p with Dandy-Walker malformation. *Prenat Diagn* **24**, 623-6 (2004).
137. Melaragno, M.I. et al. A patient with tetrasomy 9p, Dandy-Walker cyst and Hirschsprung disease. *Ann Genet* **35**, 79-84 (1992).
138. Stumm, M. et al. Mosaic tetrasomy 9p in a girl with multiple congenital anomalies: cytogenetic and molecular-cytogenetic studies. *Eur J Pediatr* **158**, 571-5 (1999).
139. Temtamy, S.A. et al. Phenotypic and cytogenetic spectrum of 9p trisomy. *Genet Couns* **18**, 29-48 (2007).
140. Hirano, H. et al. Hydrocephalus due to villous hypertrophy of the choroid plexus in the lateral ventricles. Case report. *J Neurosurg* **80**, 321-3 (1994).
141. Welch, K., Strand, R., Bresnan, M. & Cavazzuti, V. Congenital hydrocephalus due to villous hypertrophy of the telencephalic choroid plexuses. Case report. *J Neurosurg* **59**, 172-5 (1983).
142. Fujimura, M. et al. Hydrocephalus due to cerebrospinal fluid overproduction by bilateral choroid plexus papillomas. *Childs Nerv Syst* **20**, 485-8 (2004).
143. Rickert, C.H., Wiestler, O.D. & Paulus, W. Chromosomal imbalances in choroid plexus tumors. *Am J Pathol* **160**, 1105-13 (2002).
144. Grill, J. et al. Comparative genomic hybridization detects specific cytogenetic abnormalities in pediatric ependymomas and choroid plexus papillomas. *Cancer Genet Cytogenet* **136**, 121-5 (2002).
145. Sakai, J. et al. Structure, chromosome location, and expression of the human very low density lipoprotein receptor gene. *J Biol Chem* **269**, 2173-82 (1994).
146. Tacken, P.J., Hofker, M.H., Havekes, L.M. & van Dijk, K.W. Living up to a name: the role of the VLDL receptor in lipid metabolism. *Curr Opin Lipidol* **12**, 275-9 (2001).
147. Hiesberger, T. et al. Direct binding of Reelin to VLDL receptor and ApoE receptor 2 induces tyrosine phosphorylation of disabled-1 and modulates tau phosphorylation. *Neuron* **24**, 481-9 (1999).

148. Ogawa, M. et al. The reeler gene-associated antigen on Cajal-Retzius neurons is a crucial molecule for laminar organization of cortical neurons. *Neuron* **14**, 899-912 (1995).
149. Weeber, E.J. et al. Reelin and ApoE receptors cooperate to enhance hippocampal synaptic plasticity and learning. *J Biol Chem* **277**, 39944-52 (2002).
150. Niu, S., Renfro, A., Quattrocchi, C.C., Sheldon, M. & D'Arcangelo, G. Reelin promotes hippocampal dendrite development through the VLDLR/ApoER2-Dab1 pathway. *Neuron* **41**, 71-84 (2004).
151. Gong, C., Wang, T.W., Huang, H.S. & Parent, J.M. Reelin regulates neuronal progenitor migration in intact and epileptic hippocampus. *J Neurosci* **27**, 1803-11 (2007).
152. Trommsdorff, M. et al. Reeler/Disabled-like disruption of neuronal migration in knockout mice lacking the VLDL receptor and ApoE receptor 2. *Cell* **97**, 689-701 (1999).
153. Hack, I. et al. Divergent roles of ApoER2 and Vldlr in the migration of cortical neurons. *Development* **134**, 3883-91 (2007).
154. Falconer, D. Two new mutants, Trembler and 'Reeler', with neurological actions in the human mouse. *J Genetics*, 182-201 (1951).
155. Goffinet, A.M. An early development defect in the cerebral cortex of the reeler mouse. A morphological study leading to a hypothesis concerning the action of the mutant gene. *Anat Embryol (Berl)* **157**, 205-16 (1979).
156. Caviness, V.S., Jr. & Sidman, R.L. Time of origin or corresponding cell classes in the cerebral cortex of normal and reeler mutant mice: an autoradiographic analysis. *J Comp Neurol* **148**, 141-51 (1973).
157. Goffinet, A.M. Events governing organization of postmigratory neurons: studies on brain development in normal and reeler mice. *Brain Res* **319**, 261-96 (1984).
158. Goffinet, A.M. Developmental neurobiology. A real gene for reeler. *Nature* **374**, 675-6 (1995).
159. Zhang, G. et al. The Pafah1b complex interacts with the Reelin receptor VLDLR. *PLoS ONE* **2**, e252 (2007).
160. Frykman, P.K., Brown, M.S., Yamamoto, T., Goldstein, J.L. & Herz, J. Normal plasma lipoproteins and fertility in gene-targeted mice homozygous for a disruption in the gene encoding very low density lipoprotein receptor. *Proc Natl Acad Sci U S A* **92**, 8453-7 (1995).
161. Schurig, V., Orman, A.V. & Bowen, P. Nonprogressive cerebellar disorder with mental retardation and autosomal recessive inheritance in Hutterites. *Am J Med Genet* **9**, 43-53 (1981).
162. Pallister, P.D. & Opitz, J.M. Disequilibrium syndrome in Montana Hutterites. *Am J Med Genet* **22**, 567-9 (1985).
163. Tan, U. A new syndrome with quadrupedal gait, primitive speech, and severe mental retardation as a live model for human evolution. *Int J Neurosci* **116**, 361-9 (2006).
164. Ozcelik, T. et al. Reply to Herz et al. and Humphrey et al.: Genetic heterogeneity of cerebellar hypoplasia with quadrupedal locomotion. *Proc Natl Acad Sci U S A* **105**, E32-3 (2008).

165. Herz, J., Boycott, K.M. & Parboosingh, J.S. "Devolution" of bipedality. *Proc Natl Acad Sci U S A* **105**, E25 (2008).
166. Humphrey, N., Mundlos, S. & Turkmen, S. Genes and quadrupedal locomotion in humans. *Proc Natl Acad Sci U S A* **105**, E26 (2008).